ASYMMETRIC LATERAL JET INTERACTION STUDIES FOR A SUPERSONIC MISSILE: CFD PREDICTION AND COMPARISON TO FORCE AND MOMENT MEASUREMENTS

B. Srivastava
Raytheon Company
Electronics System Division
Tewksbury, MA 01876

Abstract

Computational Fluid Dynamics (CFD) predictions are compared with the wind-tunnel tests for a missile consisting of ogive-nose cylindrical body, four wings and four in-lined tail panels at nominal supersonic Mach Nos. 2, 3, 4 and 5 and at angles-of-attack ranging from 0 to 35 deg with and without a lateral jet thruster with thrust ratios of 1 and 4. Comparisons also include roll angles that lead to asymmetric missile configuration with the thruster jet. Excellent comparisons of the predicted normal force, side force, pitching moment, yawing moment and rolling moment coefficients with the measured data are shown. CFD computed flow-field is then utilized to show that the lateral thruster jet effectiveness diminishes as the jet thruster is gradually rolled towards the windward side of the missile. Flow-physics associated with this phenomenon and possible mechanisms to alleviate this effect is discussed.

Nomenclature

AF	Amplification Factor, $1 + (CN_{jet} - CN_{no\text{-}jet})/(T/q \bullet S)$
Alpha	Angle-of-Attack (deg)
Clm	Rolling Moment Coefficient, $Mx/(q \bullet S \bullet X_{ref})$
Cm	Pitching Moment Coefficient, $My/(q \bullet S \bullet X_{ref})$
CN	Normal Force Coefficient, CN = (N/q • S), Airframe only
CY	Side Force Coefficient, FY/(q • S)
CYm	Yawing Moment Coefficient, $Mz/(q \bullet S \bullet X_{ref})$
dp	Pressure Differential, $dp = (P_{jet} - P_{no\text{-}jet})/(Gamma \bullet P_{inf})$
Gamma	Ratio of Specific Heats
FY	Side Force (N, lb)
M	Freestream Mach Number
Mx	Rolling Moment
My	Pitching Moment
Mz	Yawing Moment
N	Normal Force (N, lb)
P	Pressure (N/m^2, lb/ft^2)
Phi	Azimuth Angle (deg)
q	Dynamic Pressure, $q = 1/2\ \rho v^2$
S	Missile Cross-Sectional Area (m^2, ft^2)
T	Jet Thrust (N, lb)
v	Velocity (m/sec, ft/sec)

Greek

α	Angle-of-Attack (deg)
ρ	Density
ϕ	Azimuth Angle (deg)

Subscript

inf	Freestream condition
jet	Condition with jet (excluding Jet Thrust Coefficient)
no-jet	Condition with no jet
X_{ref}	Reference Length for Normalization

Introduction

For short range air-to-air missiles, high maneuver requirements at launch and in the homing phase (terminal engagement) is necessary for tactical advantage in air combat engagements. Missile maneuvers up to 60 to 90 deg may be required to defend against threats. Conventional methods of improving the aerodynamic control maneuver are limited due to the weight and drag requirements of the overall missile. Advanced concepts are currently under study for enhancing the high angle-of-attack performance of the current and next generation missiles. Reaction control jets may be ideal for such applications due to its rapid response time as well as its ability to perform at all speeds and altitudes. Additional benefits include reduced size of wings and fins that can overcome the weight penalty of the reaction control system. Similar benefits are likely for surface-to-air combat scenario.

A successful effort based on the reaction jet controls, however, must develop a rational basis for such design factors as the jet size, locations, number of jets, thrust levels, effect of jet temperature, jet angle and most importantly its interaction with the missile external flow. The problem of jet interaction with the external flow, under conditions of varying flight numbers and angles-of-attack, is extremely complex in nature and an understanding of this interaction is important to achieve optimal missile performance. A large volume of experimental and analytical studies related to lateral jets dating back to the sixties are currently available in the literature. However, in spite of these studies, numerous related issues need to be addressed.

Due to the complexity of the flow involved in this interaction process, a viable approach to address some of these issues is to judiciously combine the wind tunnel testing and CFD simulations to evolve a validated design and analysis tool. The former provides a valuable data base for CFD validation while the latter provides a means for parametric design evaluation. This approach also offers a methodology to synthesize the physical complexity of the flow in an effort to identify the key controlling parameters by sequentially increasing the physical complexity of the model in a CFD simulation. At Raytheon, our design team has adopted this approach, i.e., scaled model testing, CFD validation, and design trade-off studies using validated CFD tools.

Our previous efforts for this topic dealt with CFD simulation and validation for a symmetric missile with wings and tail panels at several (17) flow conditions corresponding to the wind-tunnel tests[1,2,3,4]. More specifically, validations were performed at a nominal Mach Number of 3.94, angles-of-attack ranging from 2 to 25 deg, three different wing planforms and lateral jet thrust ratios of 1 and 4. These studies show excellent comparisons of the CFD predicted normal force and pitching moment coefficients with the wind-tunnel data. For symmetric cases, need however, exists to extend the validation range to other supersonic Mach Number e.g., 2 to 5 and higher angles-of-attack e.g., to 75 deg. Likewise, validations for asymmetric missile orientations for similar Mach Number and angles-of-attack range need to be performed to establish a credible design and analysis tool.

The present paper deals with several additional validation studies corresponding to the wind-tunnel tests, specifically for asymmetric missile orientations with and without lateral jets. A total of 16 symmetric wind-tunnel cases and an additional 17 asymmetric wind-tunnel cases are compared with the CFD predictions. The computational results with reaction jets are then analyzed to show that the reaction jets do not perform well in the windward orientation. In this orientation, the intense interaction between the incoming freestream and the jet causes a blockage effect that wipes out the normal forces on the windward wing and tail panels leading to deterioration of the missile performance. Possible design variations that can circumvent this deficiency associated with the reaction jets are outlined.

The paper is divided in several sections. The next section briefly outlines the previous work in this area using CFD approaches. The details of the computational methodology, geometry, grid related issues and boundary conditions of the CFD applications are discussed later. Our previous paper[2] presented a large number of validation cases with the wind-tunnel data with and without divert thrusters. Further validation cases at several Mach Numbers for symmetric and asymmetric missile configurations are discussed in the section that follows. The bulk of the technical discussion related to the effect of divert thruster location on the missile performance is discussed in the section after this. A later section presents the summary and conclusions based on these computational studies.

Background

The topic of jet interaction with an external supersonic flow dates back to the mid-1960[5,6], when a large number of generic experimental data were generated and related correlation techniques were developed. Emergence of hypersonic interceptors, maturity of CFD and the advent of supercomputers revived these activities in the late 1980s[7-11]. Several investigators have performed CFD studies for the fundamental problem of jet interaction in relation to adaptive gridding[12], turbulence models[13], grid refinements[14], and the impact of artificial viscosity[12]. These studies range from Euler[15] to Navier-Stokes computations[16]. Of these studies, particular reference is made to the studies reported by Dash et.al.[16] and York et.al.[10] because much of the current CFD effort is derived from their mature technical expertise in this area. Further details of the methodology and related research work can be obtained from the references cited.

While a vast number of numerical studies have been performed using controlled jet interaction studies for methodology development, efforts to simulate missile surfaces have been rather limited. More recently, Chan et.al.[17] performed a series of studies that lead to the simulation of a full missile surface with control surfaces and jet interaction. Qin and Foster[18] also performed similar studies using a Navier-Stokes approach for an inclined jet on an ogive/cylinder body. These results depict the remarkable flow details obtained using CFD approaches, which ultimately result in making judicious choices for flight vehicles design and further wind tunnel testing. Srivastava[3] performed Full Navier-Stokes (FNS) studies for generic missile bodies with/without leeward and windward jets but without wing or tail panels. Comparisons with the wind-tunnel data, however, was not direct because the tests were conducted with tail panels while computations were performed without tail. Removal of the tail load from the wind-tunnel data by an approximate method introduced uncertainties that were

not fully quantified. This deficiency in the CFD model was eliminated later by Srivastava[4] showing direct comparison of the CFD predictions with the wind-tunnel data by modeling all geometrical aspects of the wind-tunnel missile geometry and the divert thruster.

Computational Methodology

PARCH[10], which is a FNS code with plume/missile airframe steady-flow predictive capability, is being used for our current studies. PARCH code utilizes formulations based on the NASA/Ames ARC aerodynamic code and the AEDC propulsive extension, PARC. This code is particularly suited for missile surfaces due to its grid patching capability which is useful for treating embedded surfaces in a flow field. Patching, that is accomplished in mapped computational coordinates, is automatically constructed from boundary inputs. Boundary conditions are applied along the outer computational boundaries and relevant embedded surfaces. The code utilizes diagonalized Beam-Warming numerics with matrix-split finite rate chemistry. Several versions of the K-E turbulence model are available in the code that were specifically developed for jet interaction and propulsive studies. We are currently using the capped low Reynolds number formulation of Chien's K-E model[16] for the current simulations. Further details of the code capability can be found in Reference 10.

Typical boundary approaches for the current application (supersonic flows) are specified supersonic freestream conditions at the inlet and outer boundaries. Extrapolation procedures are employed at the exit boundary. Surface conditions are appropriate to viscous flows with adiabatic wall condition.

Surface jet boundary condition is the specified jet nozzle supersonic exit conditions. The circular area of the jet in the wind-tunnel test is approximated by a square aperture in the CFD simulation.

Fig. (1) shows a sketch of a generic Missile geometry. The wing in Fig. (1) is the baseline configuration which is 6.3 body diameters long and its leading edge starts at 4.85 body diameters from the missile nose. The jet thruster is located at 5.6 body diameters from the nose. The full CFD simulation geometry is shown in Fig. (2) for this configuration.

CFD simulations were performed on a single grid consisting of 230*51*137 axial, normal and circumferential grid. A grid patching procedure was used to apply the relevant boundary conditions on the surfaces. All angles-of-attack for a given configuration were simulated on a single grid consistent with the minimum desired Mach Number and maximum desired angle-of-attack. This allows us to minimize on the grid effort. The grids were generated through "GRIDGEN", with geometry models developed within "GRIDGEN"[19].

Our current studies for divert jet were performed for a nominal flow Mach Number of 4 with an angle-of-attack ranging from 3 to 20 deg for several peripheral jet orientations.

Comparison with Wind-Tunnel Tests

Test cases with Divert Jets

A large number of symmetric configuration test cases with divert jets were presented in our previous papers[2,3] showing excellent comparisons with the wind-tunnel data at a nominal Mach Number of 4, and an angle-of-attack of 20 deg. These comparisons were restricted to symmetric cases due to limited availability of the computing resources. It has now been possible to simulate the asymmetric configuration using parallel processing on our 6-Processor Digital Alpha-8400 computing resources. These results are discussed next.

Asymmetric cases

Asymmetric test cases were performed at the same nominal Mach Number of 4.0 and an angle-of-attack of 20 deg. Divert jet location was kept fixed with missile rolled around its axis to achieve several different location of the divert jet relative to the freestream. The results for these cases for a jet thrust of 175 lbs and 50 lbs are presented next.

175 lbs Jet Thrust Cases

Figs. (3) to (8) show the comparisons of the CFD results with the wind-tunnel data for several roll angles which represent divert jets in windward to leeward orientations. Fig. (3) shows the computed results for a case that is rolled by about 181.33 deg clockwise from the vertical axis, such that the jet center line makes an angle of 136.62 deg as shown in this figure. This orientation is nearly a plus configuration with a windward jet orientation. This figure shows the pressure distribution on the jet center plane (a plane surface normal to the body and passing through the jet on the wind side) and on the missile surfaces such as body, wing and tail panels. In this view, an observer is placed between the positive y-axis and the jet center line. Notice

from this figure that due to the intense interaction between the jet and the freestream, the jet streams make a parabolic shape away from the missile surfaces and in the process create a blockage effect that wipes out the favorable pressure on the windward wings. The table in this figure shows the comparison of the computed results with the wind-tunnel data for all the force and moment coefficients. The excellent comparisons are noteworthy.

Fig. (4) shows a computation with missile rolled by 136.14 deg such that the divert jet is now positioned at an angle of 91.14 deg from the vertical axis, a side thrust situation. The pressure contours are once again on a plane containing the jet and the missile surfaces. In this view, the observer is looking from the wind side, between the two windward wing panels showing pressure load recovery of these panels from the blockage effect of the divert jet that was seen in Fig. (3). The computed force and moment coefficients, once again show excellent agreement with the data.

Fig. (5) shows a computation with missile rolled by 109.9 deg with jet center line positioned at 64.9 deg from the vertical axis, this time a leeward jet situation. The pressure contours shown in this figure show the wing and tail loads, which are free from interference of the divert jet. The comparison of the CFD predictions with the wind-tunnel data is also excellent.

Compare the results of Fig. (5) with that shown in Fig. (6). The later case is at nearly same orientation as in Fig. (5) but at a lower angle-of-attack of 9.4 deg. The pressure contours show the decline in surface loads that are also reflected in the lower force and moment coefficients. The comparisons of the CFD predicted results and the wind-tunnel data is excellent even at this lower angle-of-attack. Figs. (7) and (8) show two more cases for this thrust jet thrust level. Fig. (7) is at the nearly same angle-of-attack as in Fig. (6) (9.4 versus 9 deg) but with missile rolled to 76.17 deg. Notice that for this case, the coefficients change sign as compared to those in Fig. (6). CFD results predict all coefficients very well except roll moment coefficient. The main reason for this difference is the wind tunnel balance accuracy for moment coefficients which are projected to have measurement inaccuracies of ± 0.1. The wind-tunnel data shown in this figure is well below this limit. Fig. (8) show the computed results for a 2.3 deg angle-of-attack. Notice that the coefficients have now larger negative magnitudes which are well predicted by the CFD approach.

In summary, for this jet thrust level the CFD predictions are excellent for a large number of missile roll angles and angles-of-attack at a supersonic Mach Number of 4.0. We are currently exploring available data bases for other supersonic flow conditions.

50 lbs Jet Thrust Cases

Three more cases are discussed to show the effect of reduced jet thrust on missile performance as well as for CFD validation. Figs. (9) to (11) show these results. The computational result in Fig. (9) is for an angle-of-attack of 20 deg and a missile roll angle orientation of 108.6 deg. In this missile orientation, the jet center line makes an angle of 63.6 deg with the vertical axis. Notice a reasonably good comparison of the CFD predictions with the wind-tunnel data. These comparisons are, though, not as good as earlier cases. Causes for such differences are unknown. However, for the next case, as shown in Fig. (10) at a lower angle-of-attack of 9.8 deg, the computational predictions are again in excellent comparison with the data. Similar comparisons are seen in Fig. (11), which is at a 3.1 deg angle-of-attack. Notice that the rolling moment coefficient for this case is below the measurement accuracy and hence the comparisons for this coefficient is not suitable. CFD results for such cases are projected to be more reliable.

Test Cases without Jets

Asymmetric Cases

We have wind-tunnel data for the nominal Mach Number of 4.0 without divert jets at several missile orientations and angles-of-attack. In an effort to establish a validation base, we picked cases at missile roll angles of nearly 76 and 109 deg at 20, 10 and 3 deg angles-of-attack. These cases are similar to jet cases, even though not exact. These results are shown in Figs. (12) to (16).

Fig. (12) shows the computed results for a case with missile roll angle of 75.22 deg and an angle-of-attack of 20 deg without the divert jet. The computed pressure contours show high wing and tail loadings on the windward side, as anticipated. The overall comparisons of the CFD predictions and the wind-tunnel data is excellent, as shown in the table in this figure.

Fig. (13) shows a similar case for a missile roll angle of 109.42 deg at an angle-of-attack of 20 deg. This case can be compared to the case in Fig. (5) with a jet thrust of 175 lbs and also with the case in Fig. (9) with a jet thrust of 50 lbs. Comparative evaluation of the pressure contours highlight the effects of the divert thrust at a high and low jet thrust.

Fig. (14) shows a computation corresponding to the missile roll angle of 76.6 deg, as in Fig. (12) but at a lower angle-of-attack of 9.93 deg showing good comparisons with the data. A similar computational result is shown in Fig. (15) at a different roll angle of 110.7 deg at nearly the same angle-of-attack of 9.92 deg showing good comparisons with the data. Finally Fig. (16) shows the result at a lower angle-of-attack of 3.1 deg but a roll angle of 76.6 deg. Notice from these figures that the comparisons between the CFD predictions and the data deteriorates as the magnitudes of these quantities become small. This is consistent with the measurement accuracy issues.

Symmetric Cases for M=2, 3, 5

Additional symmetric cases without jets were computed at several other Mach Numbers i.e., M=2.0, 3.0, 4.0 and 5.0 for angles-of-attack up to 30 deg for the same missile geometry corresponding to a wind-tunnel test conducted at a different site. The computed and wind tunnel normal force and moment coefficients are tabulated in Table I. These tabulated results are plotted in Figs. (17) and (18). The computational results in these figures are plotted against the corresponding experimental values with a 45 deg line drawn to show differences between the two. Any deviation from this 45 deg line shows the degree of error between the two. These figures also contain an error bar representing ±5 percent of the local value. Notice from Fig. (17) that the normal force coefficients are predicted well within five percent of the wind-tunnel data. However, the pitching moment coefficient as seen in Fig. (18) shows larger than expected error. These differences are currently being examined primarily relative to the data base from two different wind-tunnel tests and possible model differences.

Overall Asymmetric Results

All the computational and experimental results for asymmetric cases can also be put together in a graphical and tabular form, as for the symmetric cases above. This is done in Tables II and III and Figs. (19) to (23). The computational results in these figures are again plotted against the corresponding experimental values with a 45 deg line drawn to show differences between the two. Any deviation from this 45 deg line shows the degree of error between the two. These figures also contain an error bar representing ±5 percent of the local value. These results show an excellent comparison of the computed results with the wind-tunnel data, close to around ±5 percent. There are isolated points in all figures that give larger than ±5 percent error between CFD predictions and the wind-tunnel data, as is seen from these figures. There appears to be no pattern on these differences but the overall results show excellent predictive ability of the CFD approach with and without divert jets at several angles-of-attack and roll angles. Notice also that these results for the moment predictions are significantly better than the symmetric cases discussed above.

Discussion

The results presented above encompass a large number of cases with and without jets at several angles-of-attack and missile roll angles. All of these computed cases show excellent comparisons with the wind-tunnel data allowing us to develop an understanding of the jet interaction process by examining the complex details of the computed flow field. Some of these conclusions are outlined next.

Effect of Roll Angle

Previous efforts[1,4] have discussed the jet interaction process as the missile is rolled to move the divert jet from the leeward plane to windward plane (only symmetric cases were computed before). Using the current full asymmetric simulations, those observations can now be confirmed i.e.:

(1) Normal Force Amplification factor reduces to a very low value as the missile is rolled to bring the divert jet from leeward to the windward side. This process is reversed as the roll continues to bring the divert jet from the windward to the leeward side.

(2) The physical effects that cause these phenomenon are:

(a) Blockage effect of the jet on the windward side that wipes out the windward wing and tail panel

loadings. The degree of blockage is dependent on the azimuthal location of the jet on the missile body.

(b) Jet wrap-around effect that produces unfavorable pressure on the opposite side of the missile body and lifting surfaces. These effects can be reduced by multiple jets on the missile body but its magnitude is small compared to the item in (a).

(c) Favorable high intensity pressure zone ahead of the divert jet is very narrow to circumvent the negative effects outlined above.

(d) These conclusions are now being confirmed based on a full 3-D asymmetric missile with/without divert jet simulations using CFD.

Jet Location Selection

Jet location selection, to alleviate low force amplification factor in windward orientation, is an important design parameter for the enhancement of missile performance. Based on the studies presented here, wing panels forward of the divert jet alleviates the force amplification factor but only at the cost of lost tail effectiveness (see Reference 4 for more details). We propose wing-tip mounted divert jets to alleviate all aerodynamic problems. This, however, requires an appropriate engineering development to address packaging and structural integrity issues.

Summary and Conclusions

Asymmetric missile configuration at a nominal flow Mach Number of 4.0, angles-of-attack ranging from 3 to 30 deg and several missile roll angles with and without divert jets, are studied using FNS computational methodology to show excellent comparisons of the predicted force and moment coefficients with the available wind-tunnel data. Based on these studies, several earlier observations of the jet interaction effects based on symmetric CFD simulations are confirmed. Additionally, CFD computed results were examined to first determine the causes and then recommend means to alleviate the low force amplification factors observed for windward oriented jets.

References

(1) Srivastava, B.N., " Lateral Jet Effectiveness Studies for a Missile Using Navier-Stokes Solutions", 5th Annual AIAA/BMDO Technology Readiness Conference and Exhibit, Paper # 11-08 alt, September 16-20, Eglin Air Force Base, FT. Walton Beach, FL

(2) Srivastava, B.N. " Lateral Jet Control of Supersonic Missile: CFD Predictions and Comparisons to Force and Moment Measurements", AIAA Paper # 97-0639, 35th Aerospace Sciences Meeting, Reno, Nevada, January 6-10, 1997

(3) Srivastava, B.N. " CFD Analysis and Validation for Lateral Jet Control of a Missile", AIAA Paper # 96-0288, 34th Aerospace Sciences Meeting, Reno, Nevada, 1996, Also to appear in Journal of Spacecrafts and Rockets, March, 1997

(4) Srivastava, B. N., " Lateral Jet Control of a Supersonic Missile: Computational Studies with Forward, Rear Body and Wing Tip Mounted Jets" AIAA Paper No. 97-2247 to 15th Applied Aerodynamics Conference, Atlanta, June, 1997

(5) Cassel, L.A., Davis, J.G. and Engh, D.P, "Lateral Jet Control Effectiveness Prediction for Axisymmetric Missile Configurations," U.S. Army Missile Command, Redstone Arsenal, Alabama, Report #RD-TR-68-5, June, 1968

(6) Spring, Donald, "An Experimental Investigation of the Interference Effects due to a Lateral Jet Issuing from a Body of Revolution over the Mach No. Range of 0.8 to 4.5," U.S. Army Missile Command, Redstone Arsenal, Alabama, Report #RD-TR-68-10, August, 1968

(7) Chamberlain, R., "Control Jet Interaction Flowfield Analysis," Lockheed Report LMSC F268936, Aerodynamic Investigations, Vol. 5, February, 1990

(8) Chamberlain, R., "Calculation of Three-Dimensional Jet-Interaction Flowfields," AIAA Paper 90-2099, 1990

(9) Weatherly, D., and McDonough, J., "Performance Comparisons of Navier-Stokes Codes for Simulating Three-Dimensional Hypersonic Crossflow/ Jet Interaction," AIAA Paper 91-2096, 1991

(10) York, B. J., Sinha, N., Kenzakowski, D.C. and Dash, S.M., "PARCH Code Simulation of Tactical Missile Plume/Airframe/Launch Interactions," 19th JANNAF Exhaust Plume Technology Meeting, May, 1991, CPIA PWB 568, pp. 645-674

(11) Chan, S.C. and Roger, R.P., Edwards, G.L. and Brooks, W.B., "Integrated Jet Interactions CFD Predictions and Comparison to Force and Moment Measurements for a Thruster Attitude Controlled Supersonic Missile," AIAA Paper 93-3522, 1993

(12) Lytle, J.K., Harloff, G.J. and Hsu, A.T., "Three-Dimensional Compressible Jet-in-Crossflow Calculations Using Improved Viscosity Models and Adapted Grid," AIAA Paper 90-2100, 1990

(13) Dash, S.M., Sinha, N., York, B.J., Lee, R.A., and Hosangadi, A., "On the Inclusion of Advanced Turbulence Models and Nonequilibrium Thermochemistry into State-of-the-Art CFD Codes and Their Validation," AIAA Paper 92-2764, 1992

(14) Rizzetta, D.P., "Numerical Simulation of Slot Injection into a Turbulent Supersonic Stream," AIAA Paper 92-0827, 1992

(15) Darmieux, M. and Marasaa-Poey, R., "Numerical Assessment of Aerodynamic Interactions on Missiles with Transverse Jets Control," AGARD Meeting on Computational and Experimental Assessment of Jets in Cross Flow, April, 1993

(16) Dash, S.M., York, B.J., Sinha, N., Lee, R.A., Hosangadi, A., and Kenzakowski, D.C., "Recent Developments in the Simulation of Steady and Transient Transverse Jet Interactions for Missile, Rotorcraft, and Propulsive Applications," AGARD Meeting on Computational and Experimental Assessment of Jets in Cross Flow, April, 1993

(17) Chan, S.C. and Roger, R.P, Brooks, W.B, Edwards, G.L. and Boukather, S.B., "CFD Predictions and Comparisons to Wind Tunnel Data for the Asymmetric Firing of a Forward Mounted Attitude Control Thruster," AIAA Paper #95-1895, June, 1995

(18) Qin, N. and Foster, G.W, "Study of Flow Interactions due to a Supersonic Lateral Jet Using High Resolution Navier-Stokes Solutions," AIAA 94-2151, June, 1995

(19) Steinbrenner, J.P. and Chawner, J.R., "Recent Enhancements to the GRIDGEN Structural Grid Generation System," Proceedings of the NASA Workshop on Software Systems for Surface Modeling and Grid Generation, Hampton, Virginia, April, 1992

Table I. Comparison of Normal Force and Pitching Moment Coefficient for Symmetric Cases (No Jets)

Orientation	Mach Number M	Roll Angle ϕ (deg)	Angle-of-Attack α (deg)	Comparison			
				CFD C_N	Experimental C_N	CFD C_m	Experimental C_m
+	5.00	0.00	30.0	12.23	12.83	3.10	3.68
X	5.00	45.00	20.0	6.41	6.71	4.87	3.28
X	5.00	45.00	15.0	4.31	4.33	3.13	2.79
X	5.00	45.00	10.0	2.52	2.52	2.15	2.22
X	5.00	45.00	5.0	1.13	1.05	1.16	1.41
+	5.00	0.00	35.0	15.58	16.10	2.91	4.27
+	4.00	0.00	10.0	3.01	2.94	1.87	2.37
+	4.00	0.00	30.0	13.23	13.40	2.55	3.87
+	2.00	0.00	30.0	17.10	17.33	5.50	5.94
+	2.00	0.00	10.0	4.00	4.05	2.32	2.15
+	3.00	0.00	30.0	14.36	14.88	3.83	4.62
+	3.00	0.00	10.0	3.52	3.52	2.18	2.50
X	2.00	45.00	30.0	14.74	14.49	9.70	11.51
X	2.00	45.00	10.0	3.48	3.47	3.37	3.42
X	3.00	45.00	30.0	12.82	13.05	10.05	12.33
X	3.00	45.00	10.0	3.17	3.13	2.99	3.44

Table II. Comparison of Force Coefficient for Asymmetric Cases (With/Without Jets)

Orientation	Mach Number M	Roll Angle ϕ (deg)	Angle-of-Attack α (deg)	Thrust T (lbs)	Thrust Ratio $T/(qS_{ref})$	Comparison			
						CFD C_N	Experimental C_N	CFD C_Y	Experimental C_Y
X	3.94	76.00	9.98	0.00	0.00	3.03	3.00	-0.13	-0.11
X	3.94	110.70	9.92	0.00	0.00	2.98	2.95	0.16	0.22
X	3.94	74.85	18.98	175.00	3.45	3.32	3.30	-2.25	-2.2
X	3.94	109.90	19.30	175.00	3.45	5.03	4.87	-3.5	-3.6
X	3.94	108.60	19.64	50.00	0.98	6.45	6.40	-0.88	-0.73
X	3.94	76.80	19.58	50.00	0.98	6.16	6.16	-0.95	-0.92
X	3.94	136.14	19.74	175.00	3.45	6.69	6.50	-4.03	-4.5
X	3.94	181.32	20.38	175.00	3.45	9.15	9.20	-2.3	-2.5
X	3.94	106.14	9.38	175.00	3.45	0.81	0.58	-3.4	-3.14
X	3.94	76.17	9.11	175.00	3.45	-0.69	-0.69	-2.15	-2.09
X	3.94	110.60	9.77	50.00	0.98	2.37	2.17	-0.98	-0.84
X	3.94	75.90	9.69	50.00	0.98	1.85	1.81	-0.76	-0.65
X	3.94	134.40	3.10	50.00	0.98	0.80	0.66	-1.16	-1.15
X	3.94	134.10	2.96	175.00	3.45	0.70	-0.05	-3.89	-3.91
X	3.94	74.40	2.28	175.00	3.45	-2.82	-2.93	-1.95	-1.6
X	3.94	76.60	3.12	0.00	0.00	0.79	0.78	-0.02	-0.02
X	3.94	133.30	3.12	0.00	0.00	0.75	0.77	0.0	0.02

Table III. Comparison of Moment Coefficient for Asymmetric Cases (With/Without Jets)

Orien-tation	Mach Number M	Roll Angle ϕ (deg)	Angle-of-Attack α (deg)	Thrust T (lbs)	Thrust Ratio $T/(qS_{ref})$	Comparison					
						CFD C_m	Experimental C_m	CFD C_{Ym}	Experimental C_{Ym}	CFD C_{LL}	Experimental C_{LL}
X	3.94	76.00	9.98	0.00	0.00	1.91	2.18	0.38	0.51	-0.03	-0.05
X	3.94	110.70	9.92	0.00	0.00	2.08	2.32	-0.43	-0.46	0.05	0.04
X	3.94	74.85	18.98	175.00	3.45	-6.84	-6.56	-4.62	-3.93	-0.27	-0.27
X	3.94	109.90	19.30	175.00	3.45	-1.87	-1.72	-10.90	-11.09	0.44	0.47
X	3.94	108.60	19.64	50.00	0.98	1.71	2.22	-3.85	-4.01	0.39	0.40
X	3.94	76.80	19.58	50.00	0.98	-0.11	0.65	-0.89	-0.47	-0.31	-0.26
X	3.94	136.14	19.74	175.00	3.45	5.05	5.03	-12.00	-12.26	0.34	0.26
X	3.94	181.32	20.38	175.00	3.45	13.85	13.92	-10.03	-10.37	0.43	0.43
X	3.94	106.14	9.38	175.00	3.45	-4.15	-4.92	-10.66	-9.89	0.14	0.14
X	3.94	76.17	9.11	175.00	3.45	-8.35	-8.35	-5.90	-5.09	0.02	-0.04
X	3.94	110.60	9.77	50.00	0.98	0.43	0.51	-3.60	-3.66	0.11	0.18
X	3.94	75.90	9.69	50.00	0.98	-1.19	-0.66	-1.52	-1.26	-0.02	0.03
X	3.94	134.40	3.10	50.00	0.98	0.81	0.65	-3.98	-3.84	0.01	0.04
X	3.94	134.10	2.96	175.00	3.45	0.51	-1.58	-12.37	-12.03	0.03	0.06
X	3.94	74.40	2.28	175.00	3.45	-9.93	-10.16	-5.89	-4.83	0.00	0.02
X	3.94	76.60	3.12	0.00	0.00	0.83	0.92	-0.03	0.08	0.01	0.00
X	3.94	133.30	3.12	0.00	0.00	0.91	0.98	0.01	-0.02	0.01	0.00

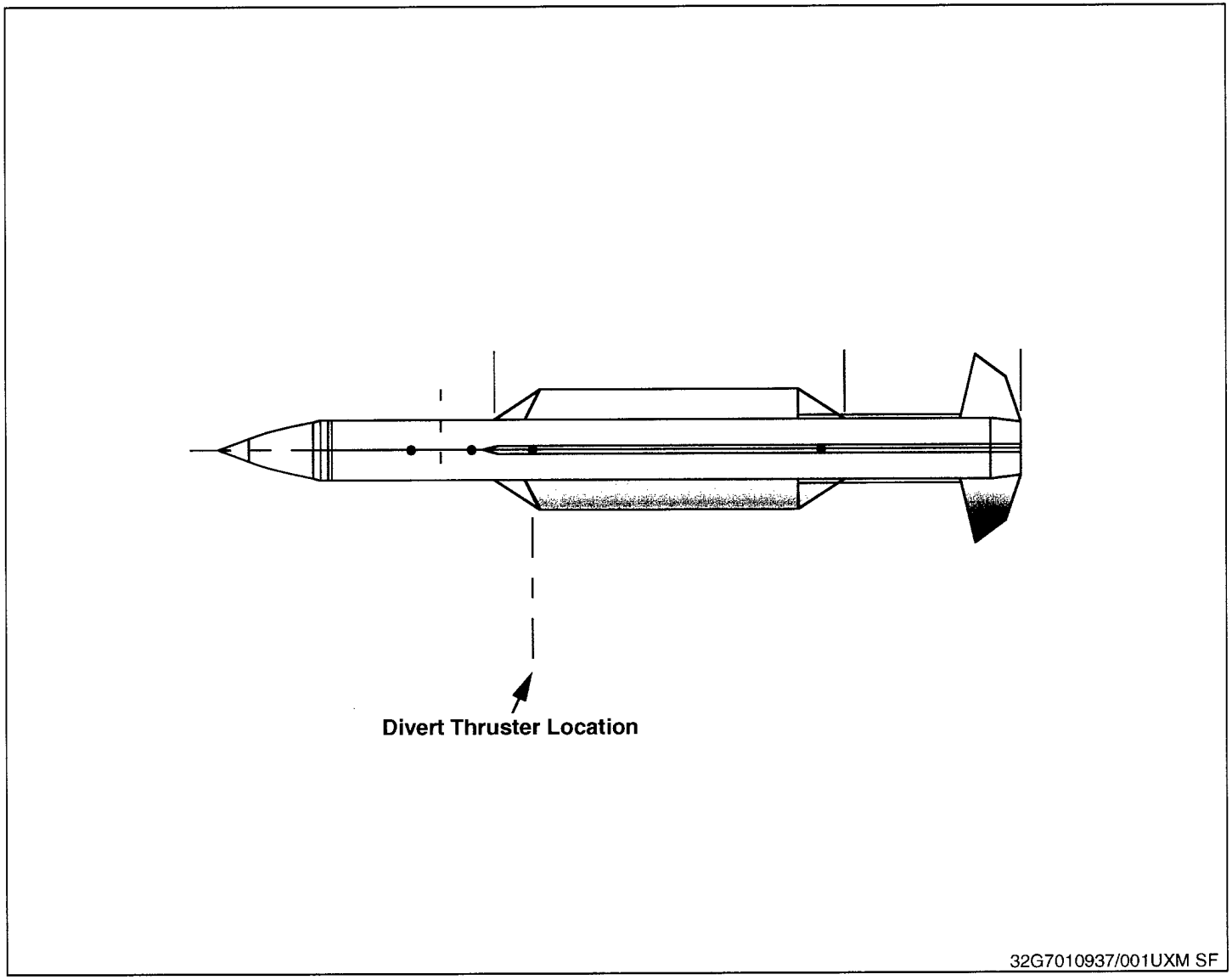

Figure 1. Geometry for CFD Simulation

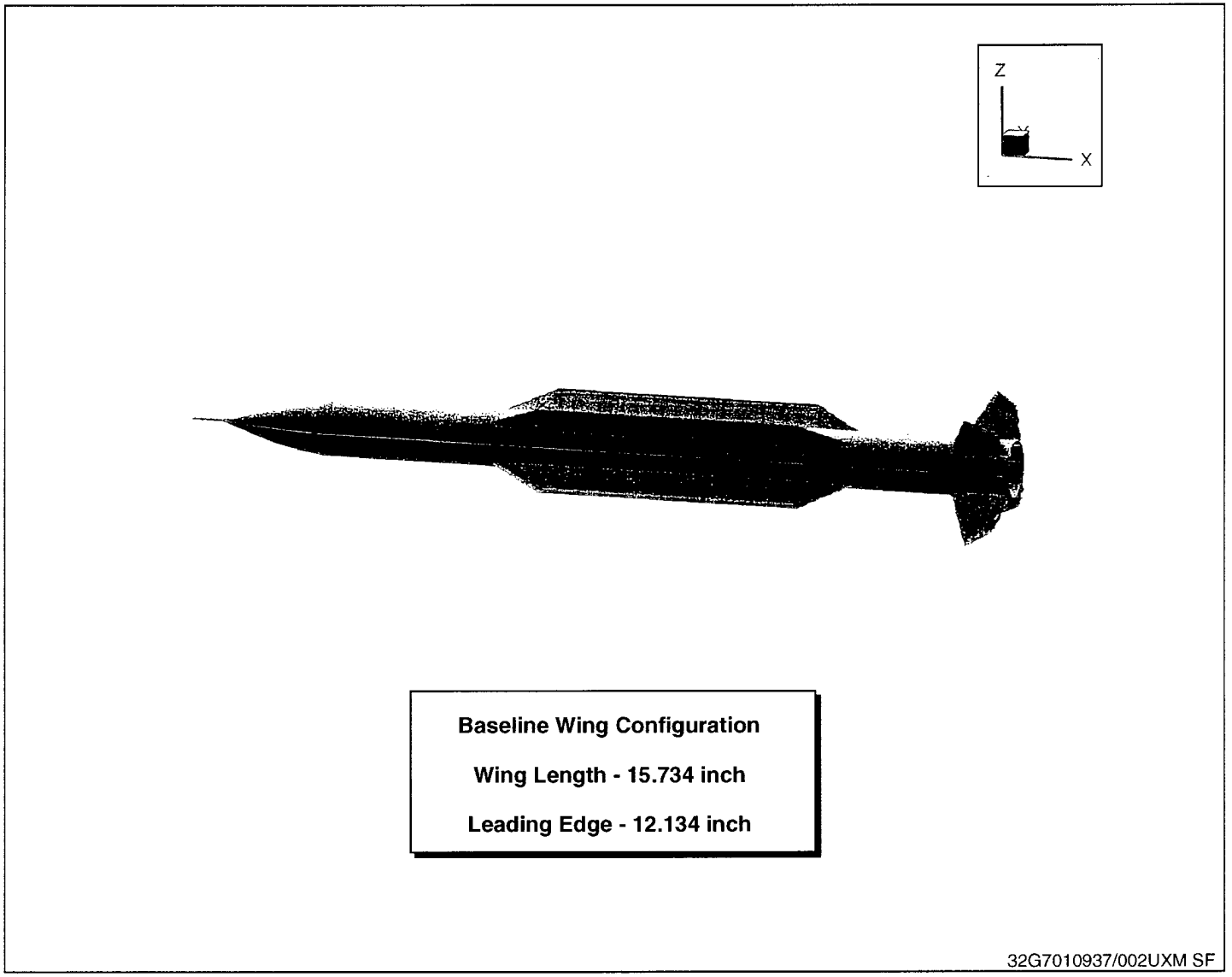

Figure 2. 3-D View of a Generic Missile

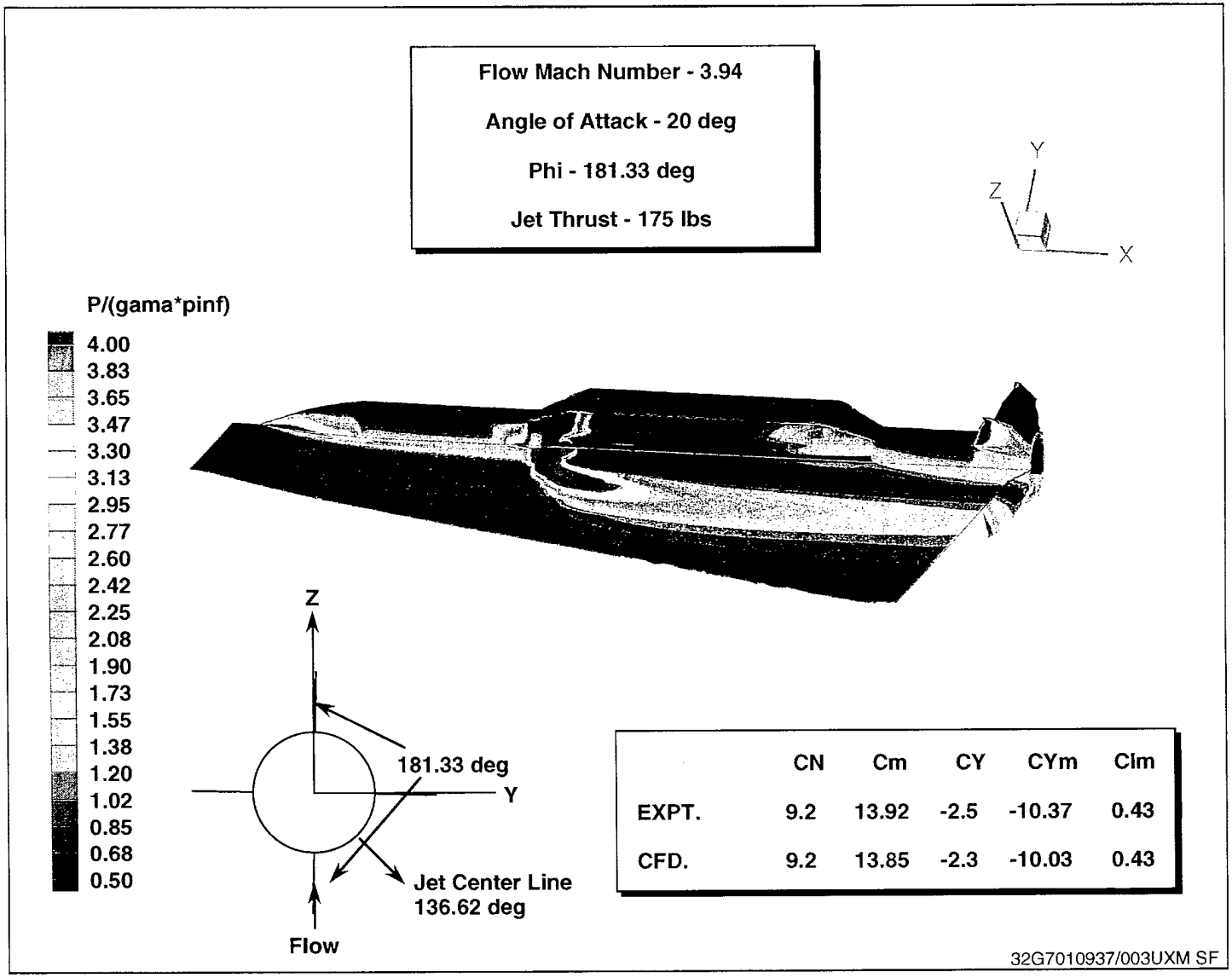

Figure 3. Pressure Distribution On Jet Center Plane and Missile Surfaces for a Windward Jet

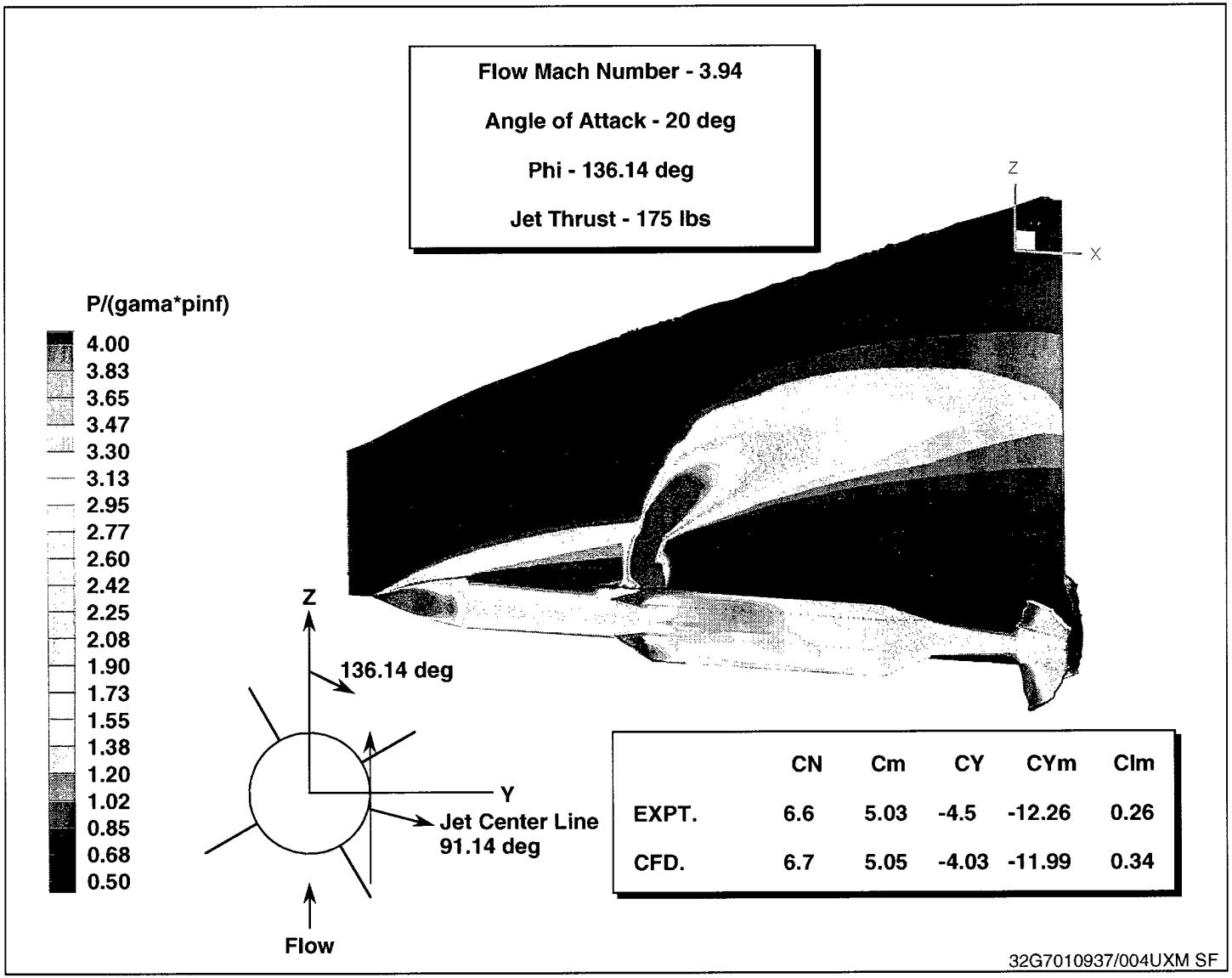

Figure 4. Pressure Distribution on Jet Center Plane and Missile Surfaces for a Side Jet

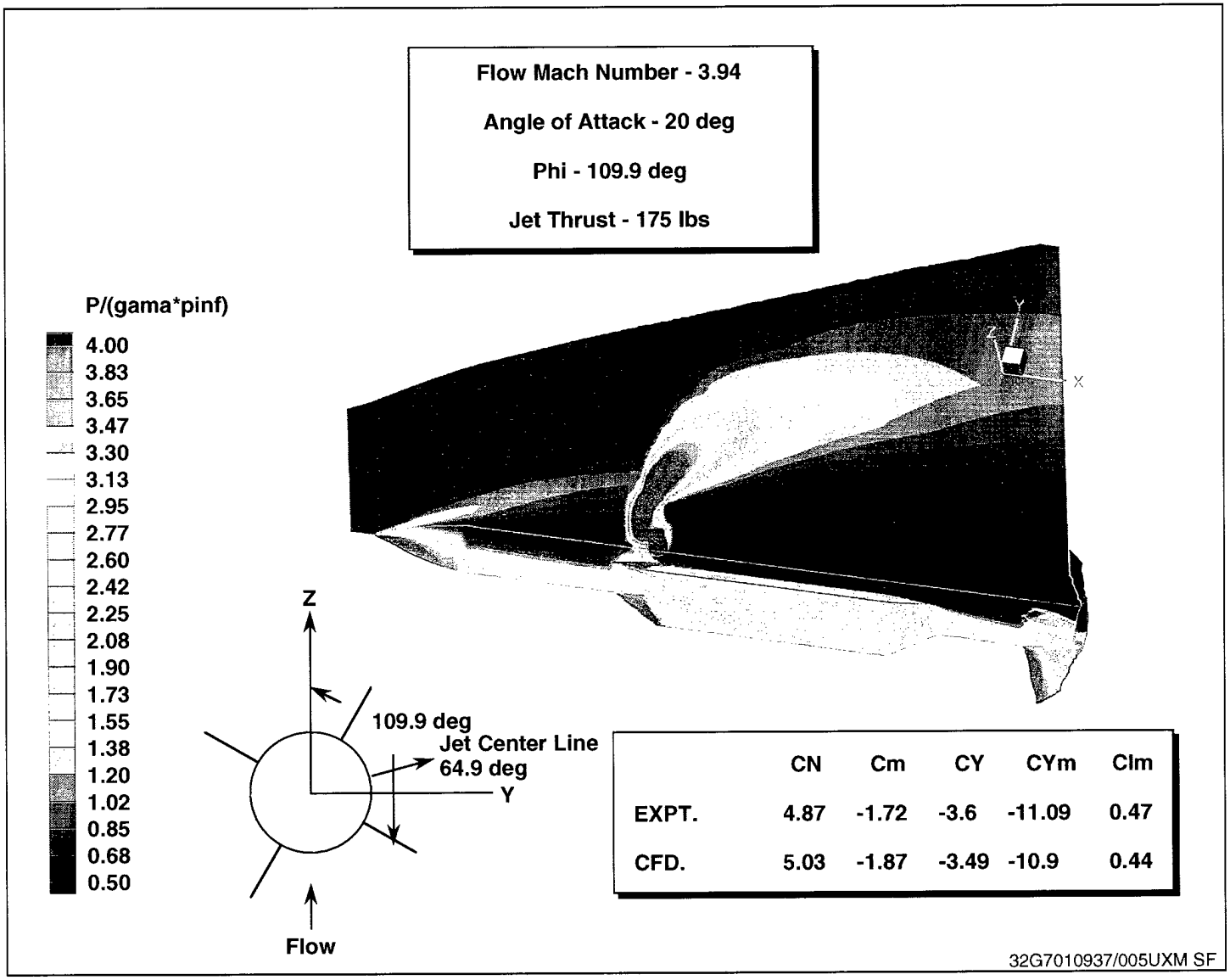

Figure 5. Pressure Distribution on Jet Center Plane and Missile Surfaces for a Leeward Jet

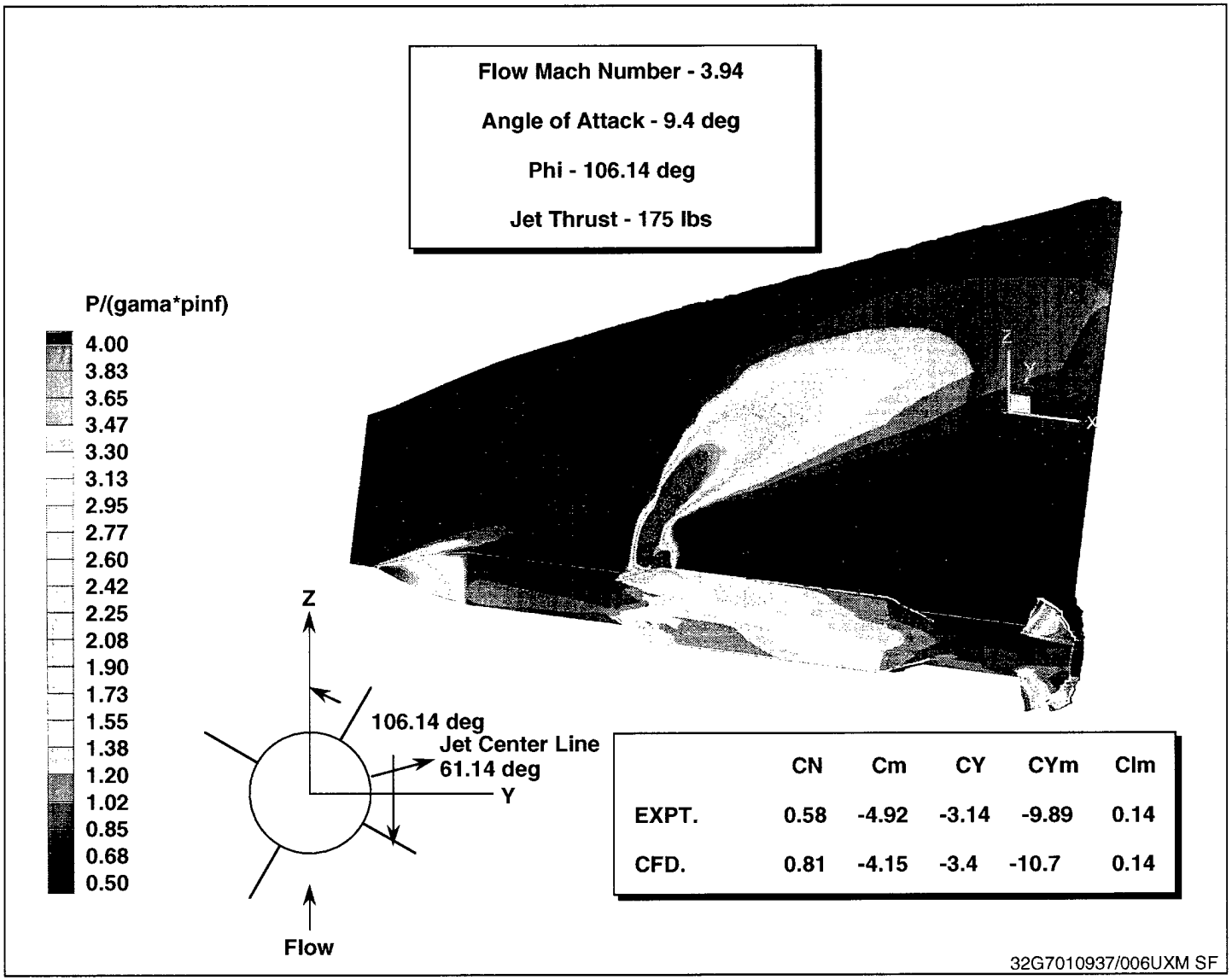

Figure 6. Pressure Distribution on Jet Center Plane and Missile Surfaces for a Leeward Jet

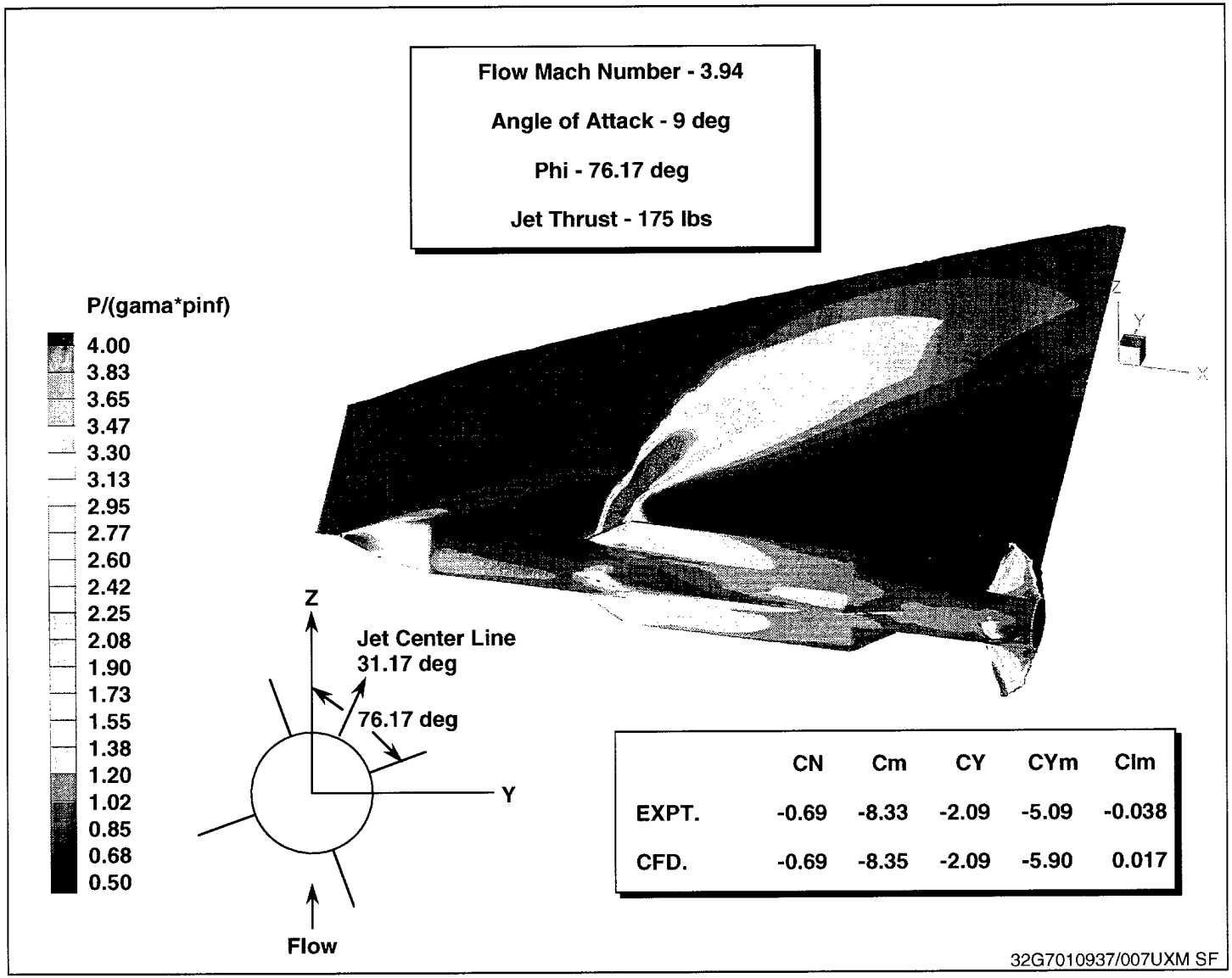

Figure 7. Pressure Distribution On Jet Center Plane and Missile Surfaces for a Leeward Jet

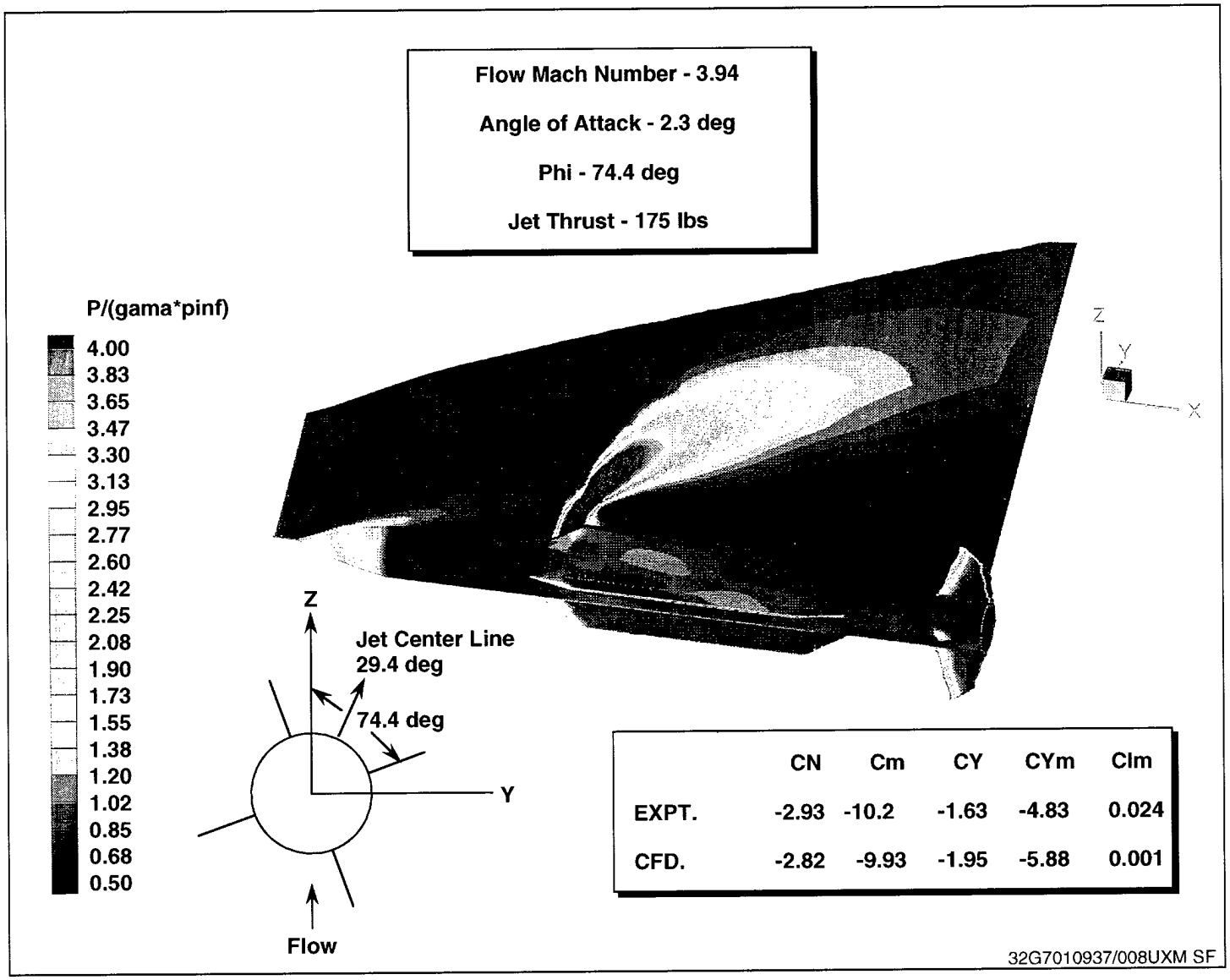

Figure 8. Pressure Distribution On Jet Center Plane and Missile Surfaces for a Leeward Jet

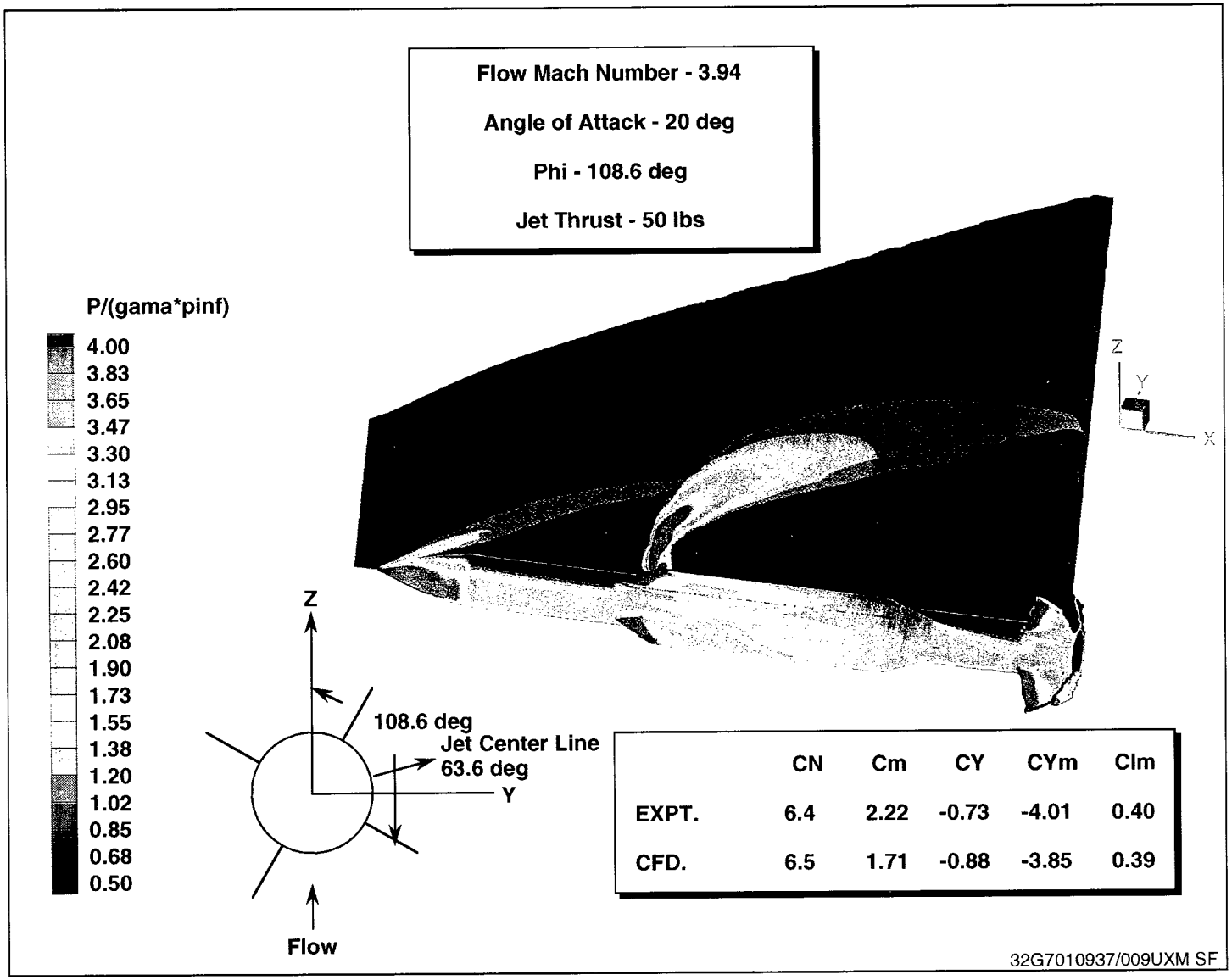

Figure 9. Pressure Distribution on Jet Center Plane and Missile Surfaces for a Leeward Jet

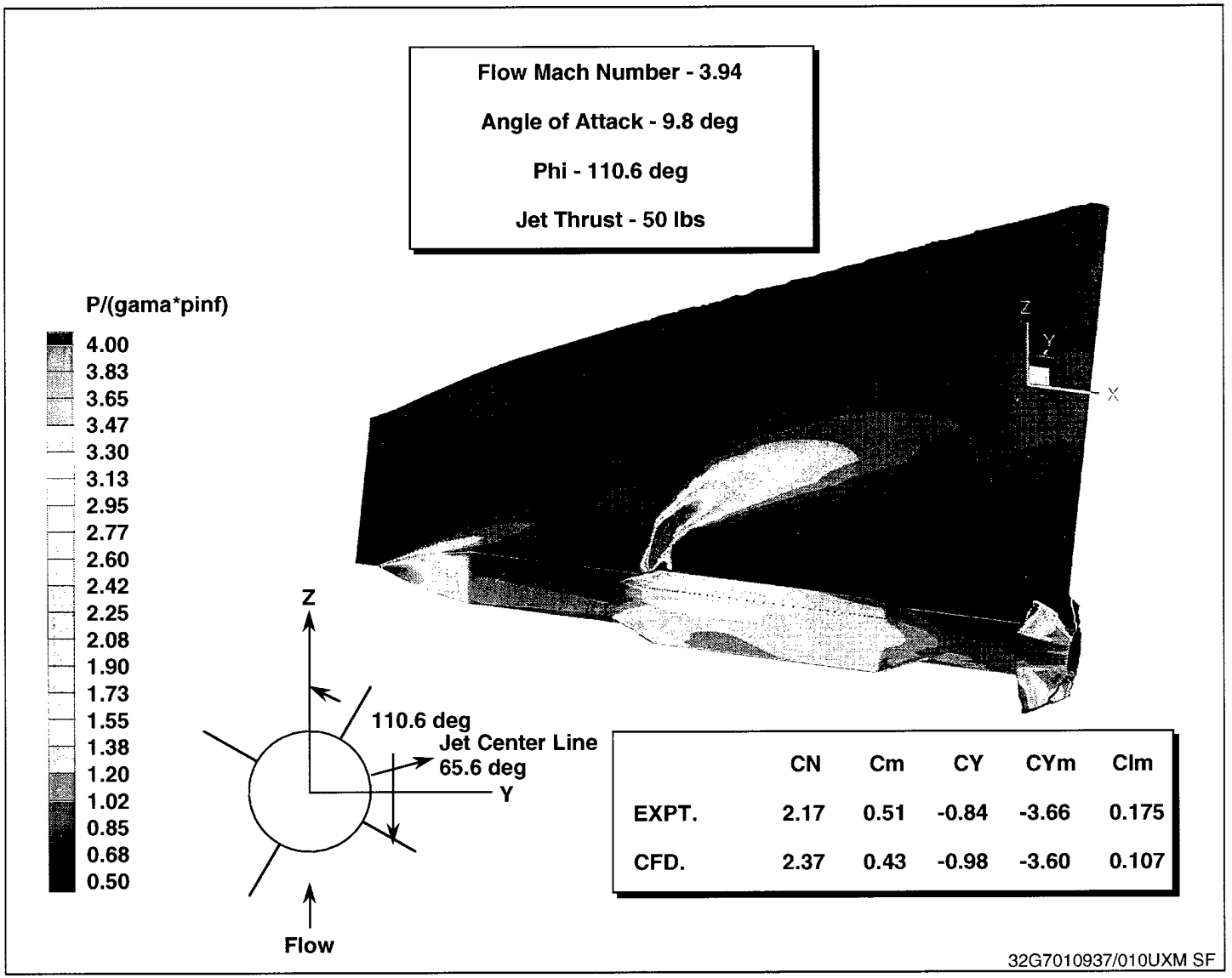

Figure 10. Pressure Distribution on Jet Center Plane and Missile Surfaces for a Leeward Jet

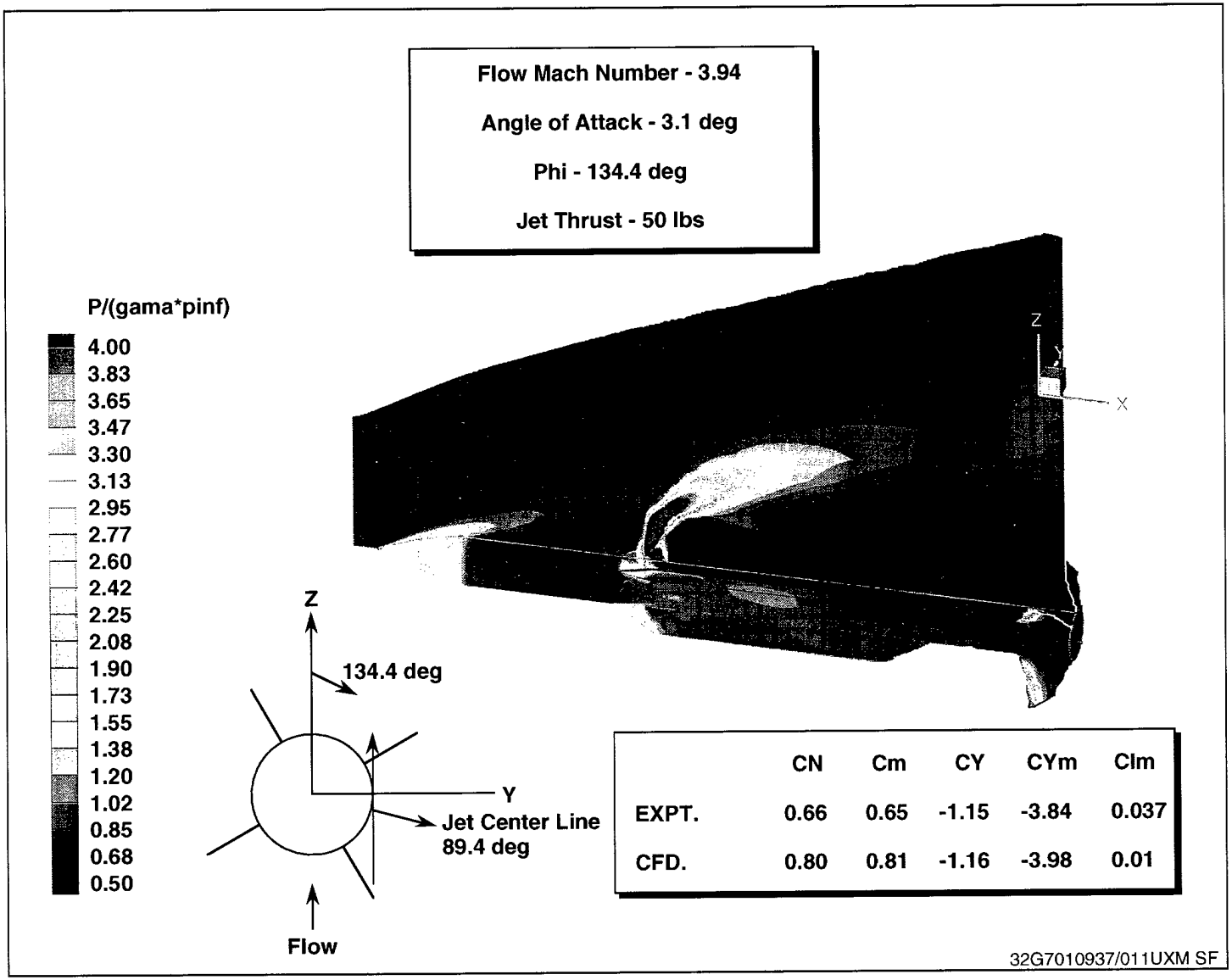

Figure 11. Pressure Distribution on Jet Center Plane and Missile Surfaces for a Side Jet

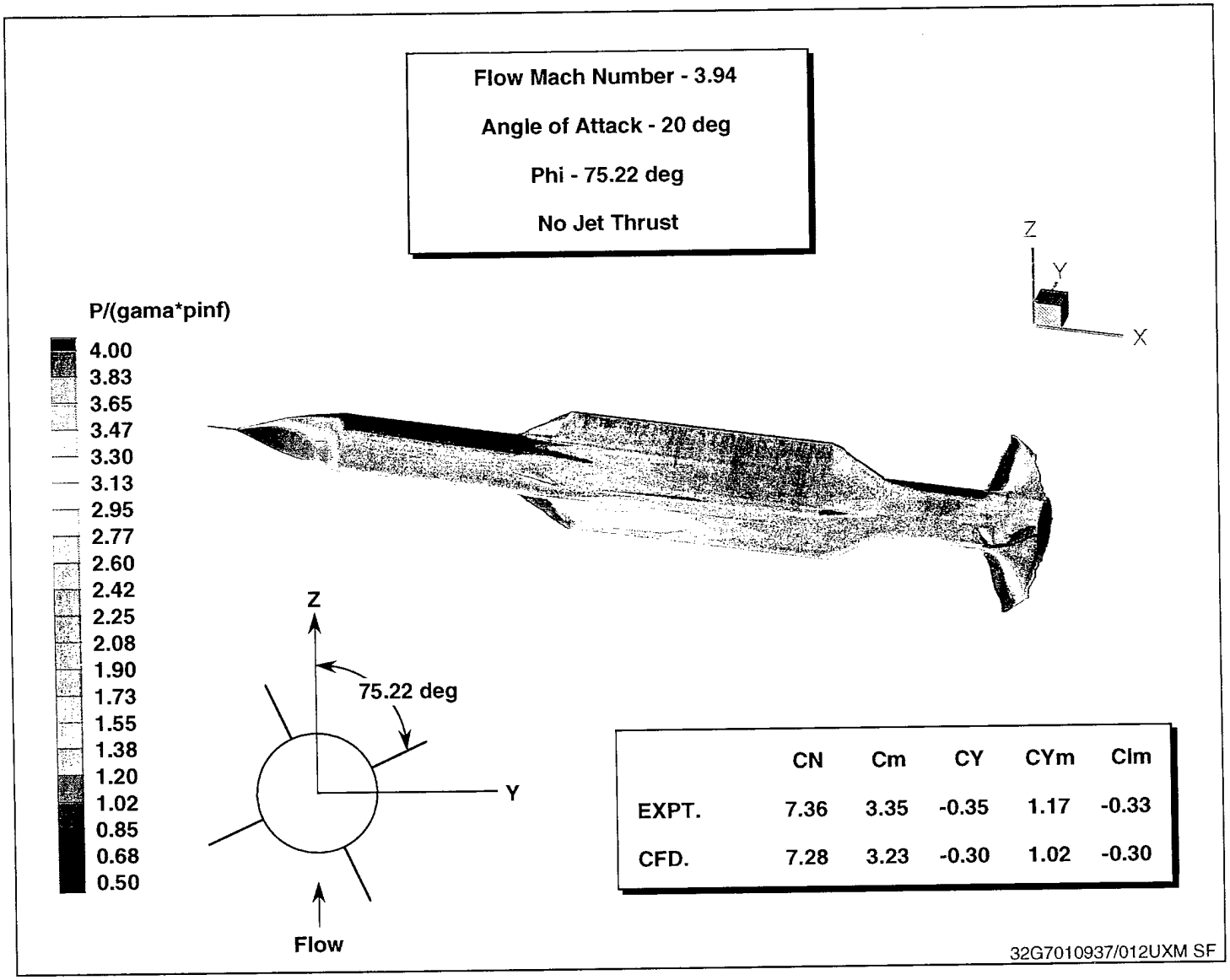

Figure 12. Pressure Distribution on Missile Surfaces for a Supersonic Asymmetric Missile Without Jet

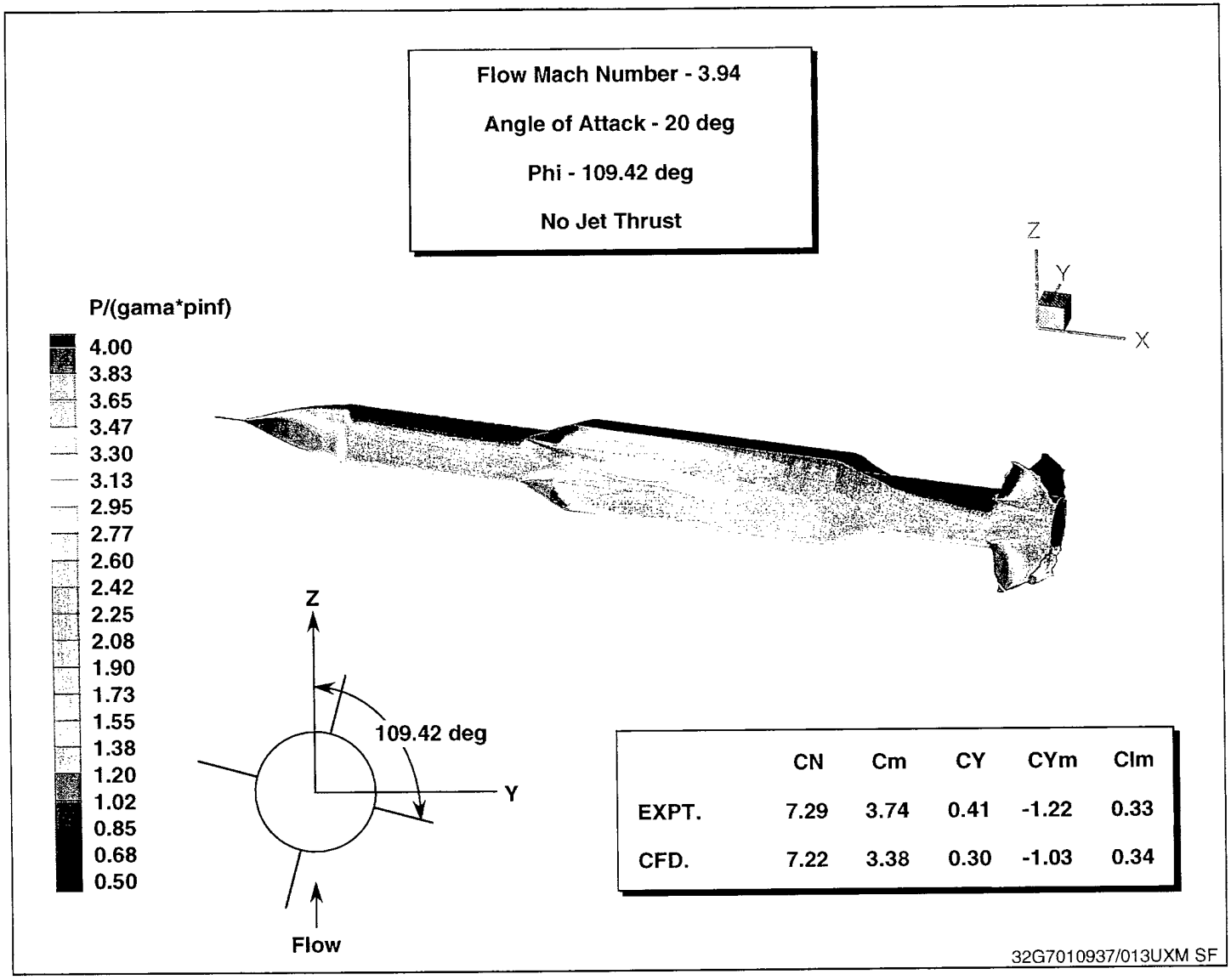

Figure 13. Pressure Distribution on Missile Surfaces for a Supersonic Asymmetric Missile Without Jet

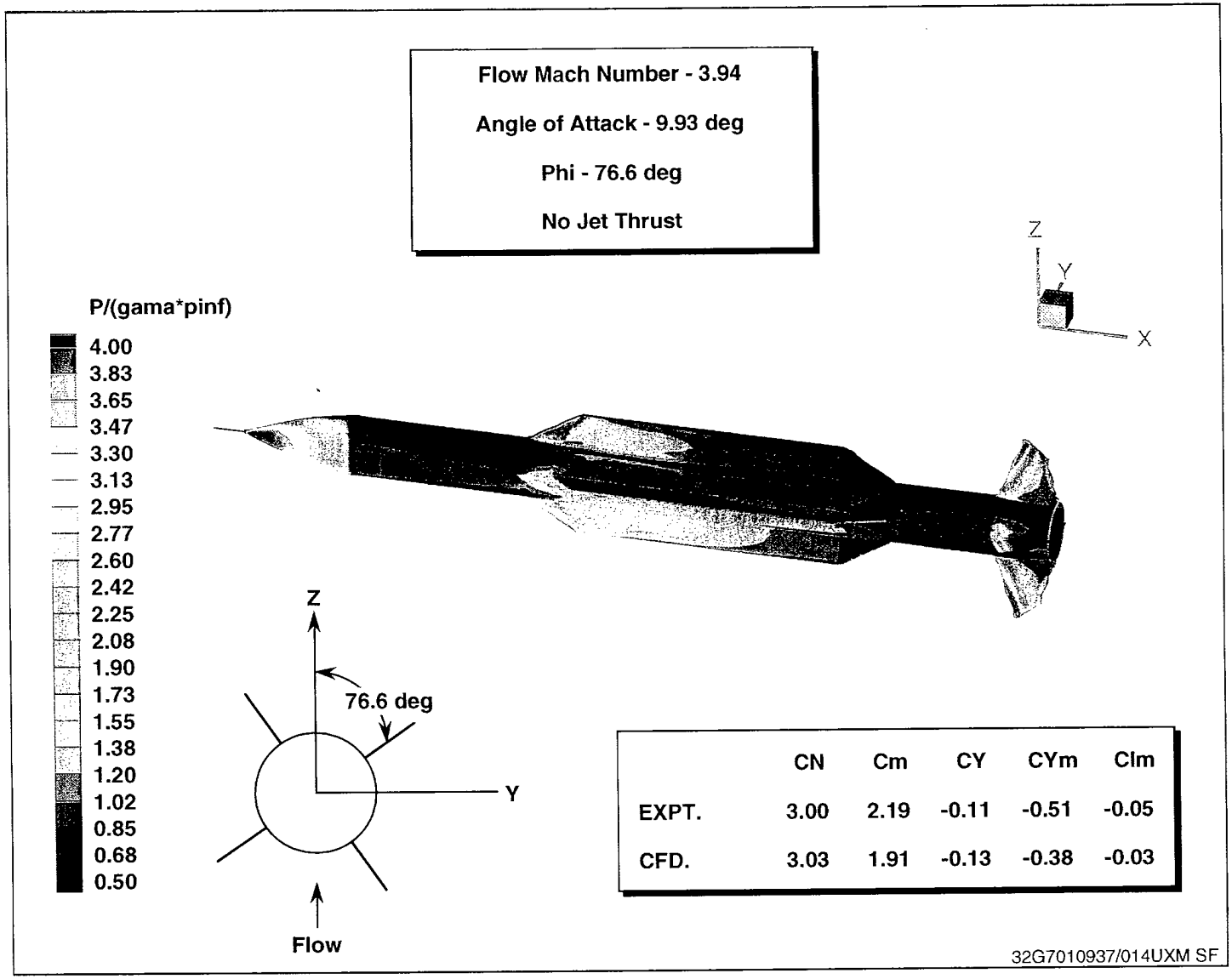

Figure 14. Pressure Distribution on Missile Surfaces for a Supersonic Asymmetric Missile Without Jet

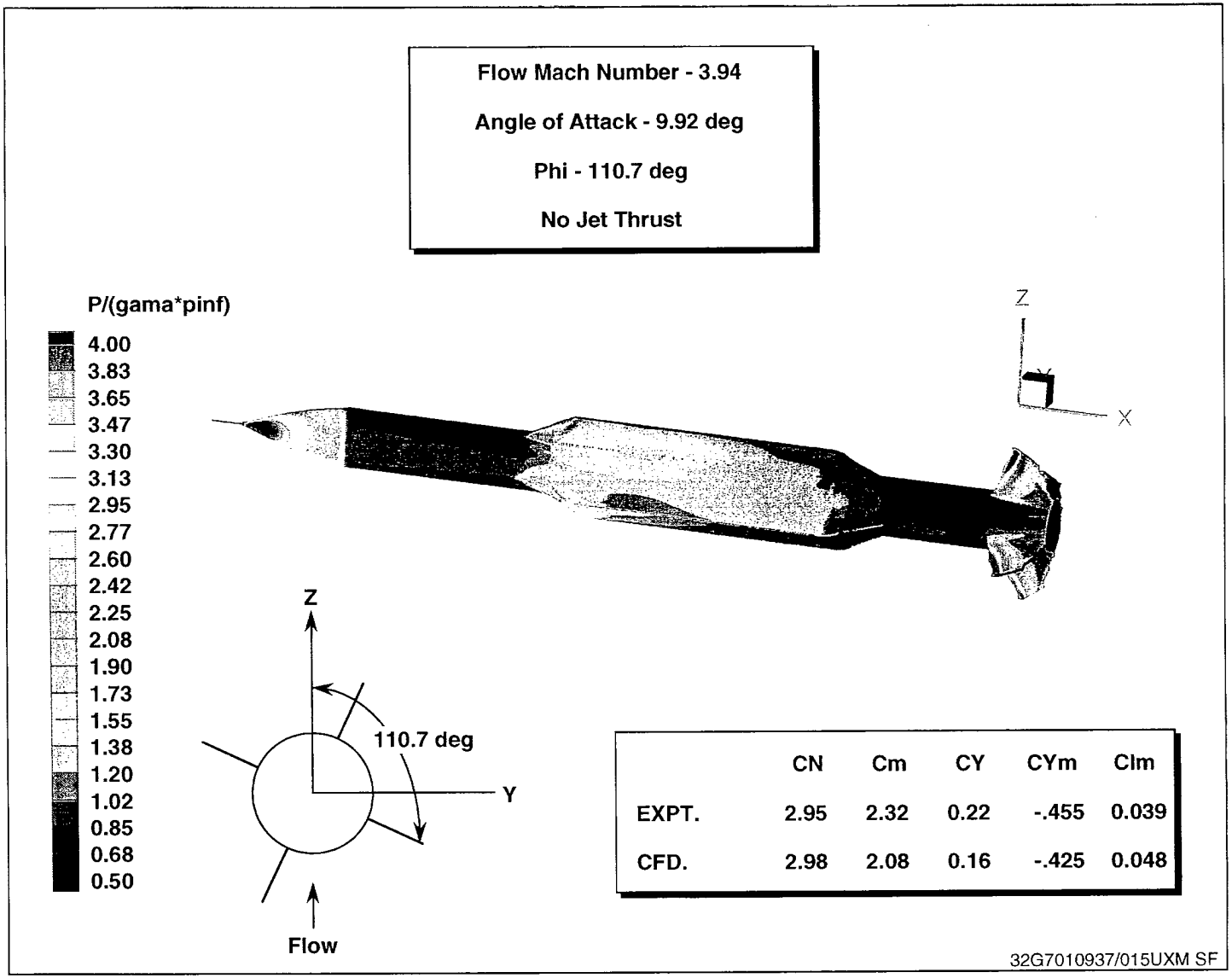

Figure 15. Pressure Distribution on Missile Surfaces for a Supersonic Asymmetric Missile Without Jet

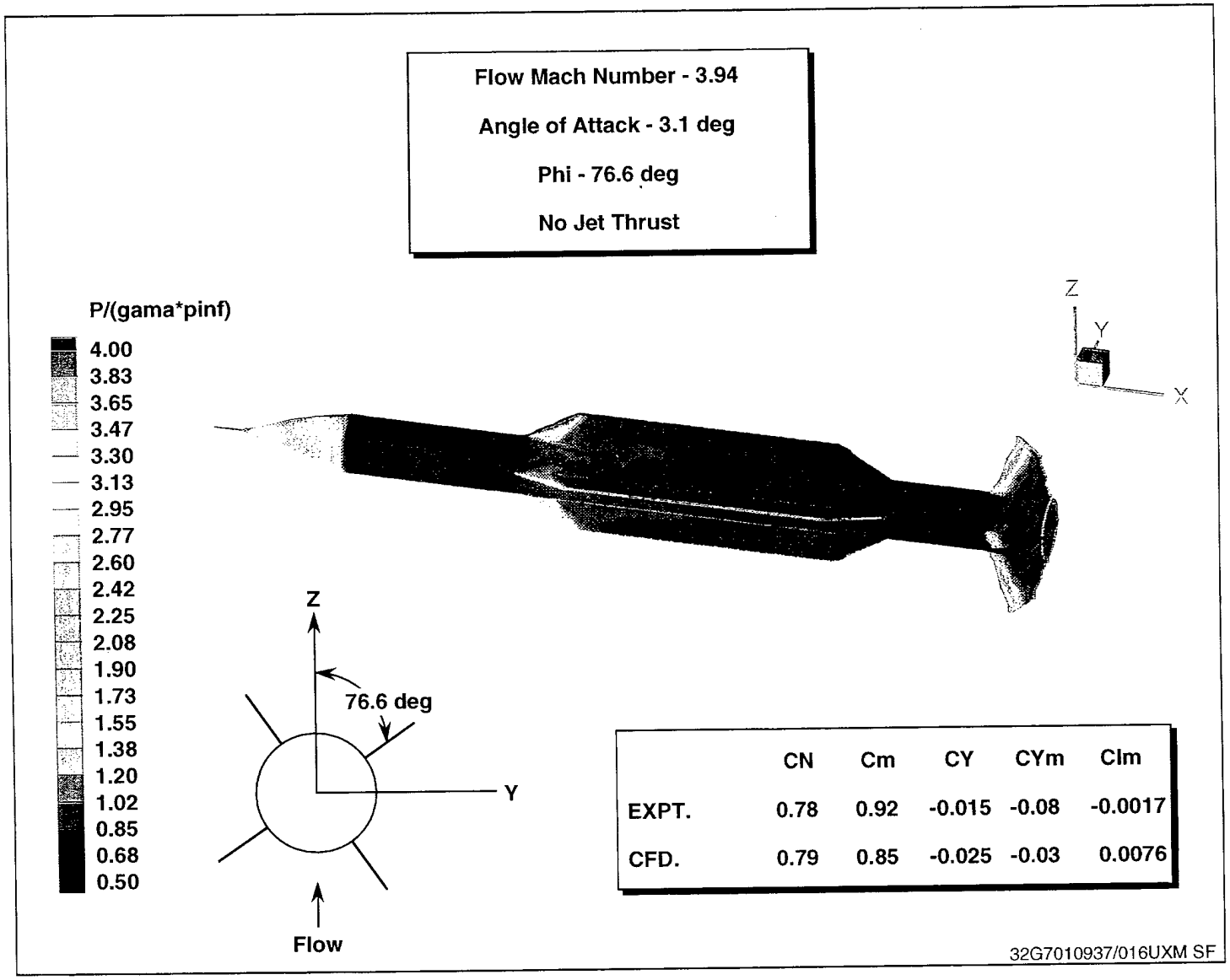

Figure 16. Pressure Distribution on Missile Surfaces for a Supersonic Asymmetric Missile Without Jet

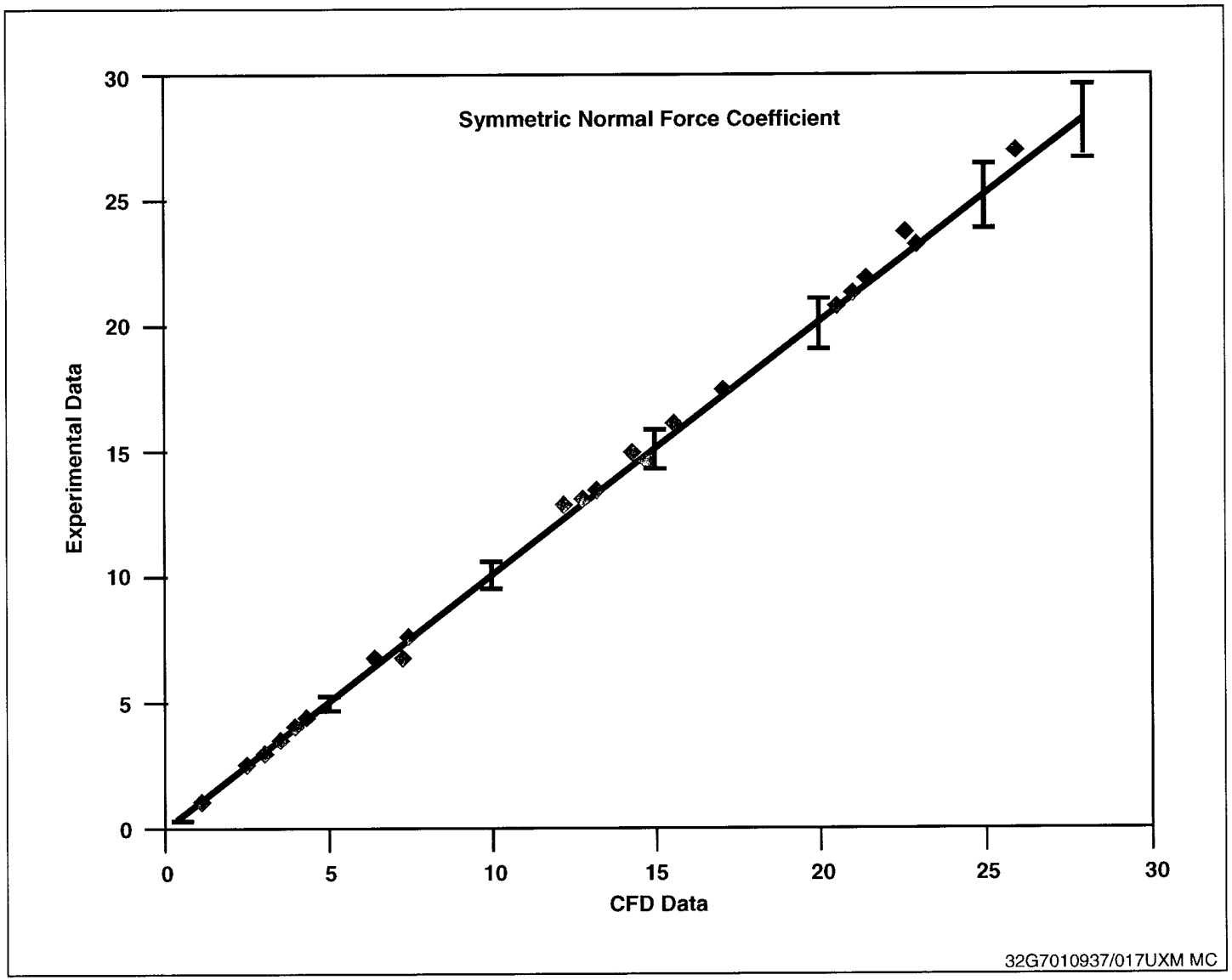

Figure 17. Comparisons of CFD and Wind Tunnel Measurements for a Symmetric Missile Configuration

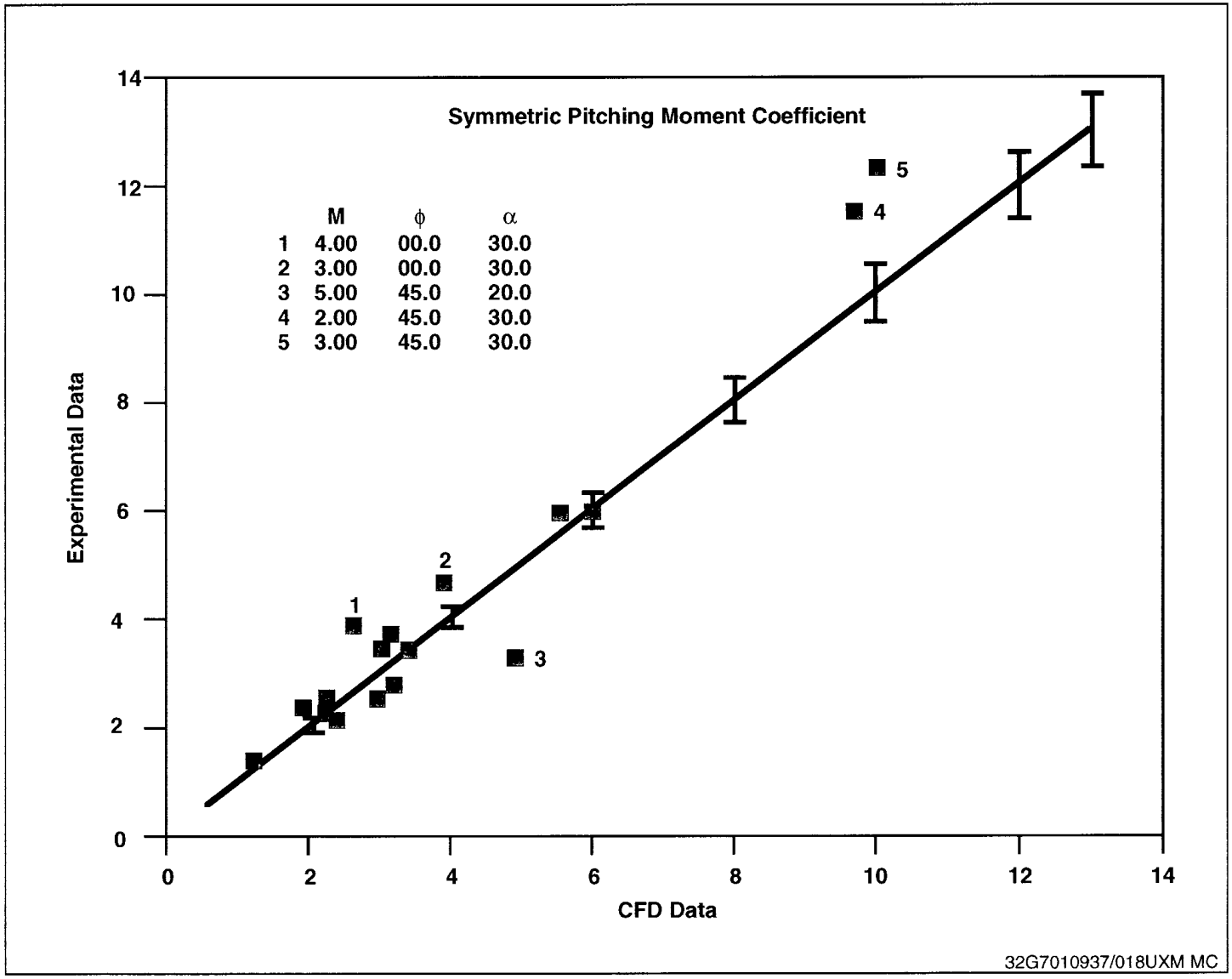

Figure 18. Comparisons of CFD and Wind Tunnel Measurements for a Symmetric Missile Configuration

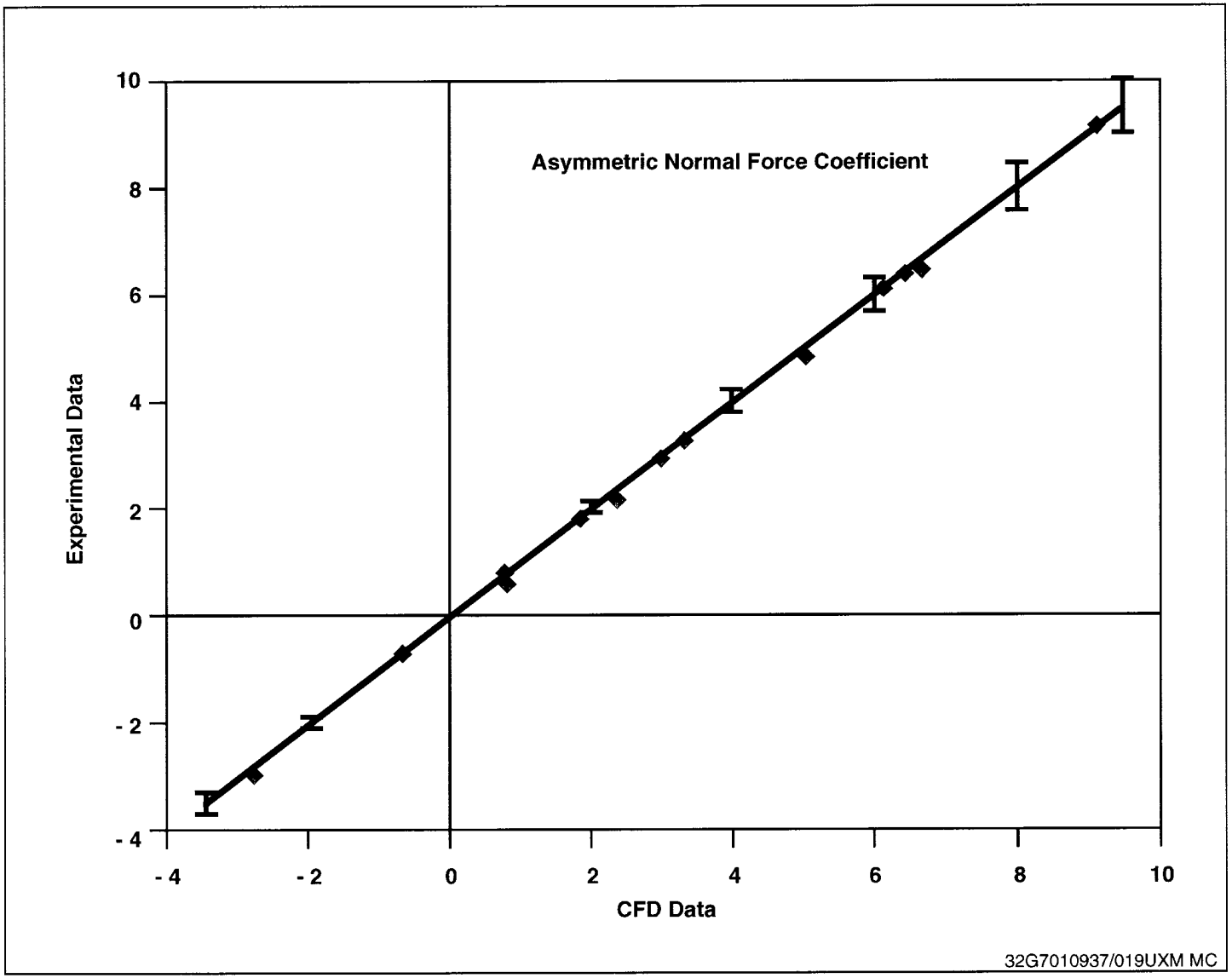

Figure 19. Comparisons of CFD and Wind Tunnel Measurements for an Asymmetric Missile Configuration

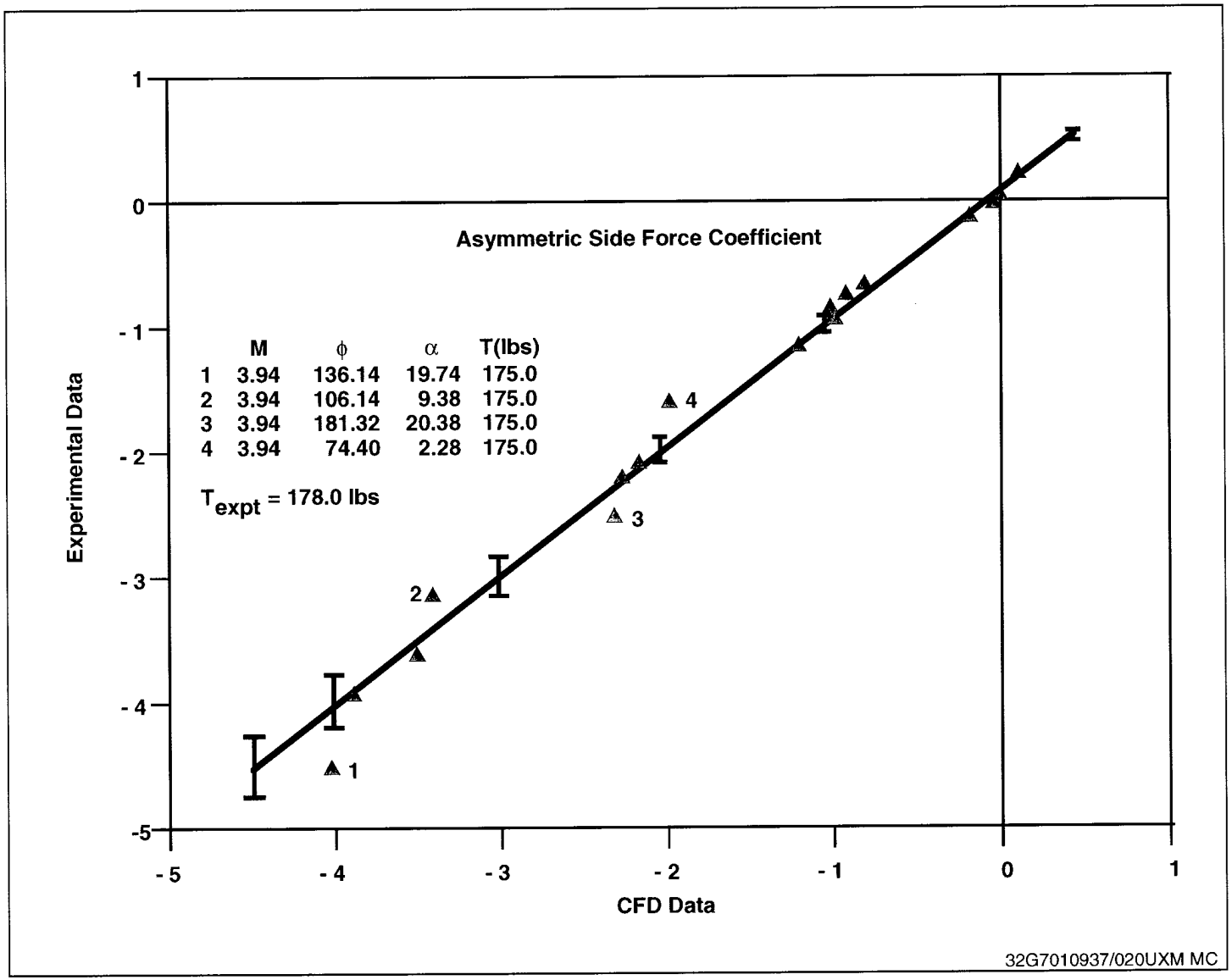

Figure 20. Comparisons of CFD and Wind Tunnel Measurements for an Asymmetric Missile Configuration

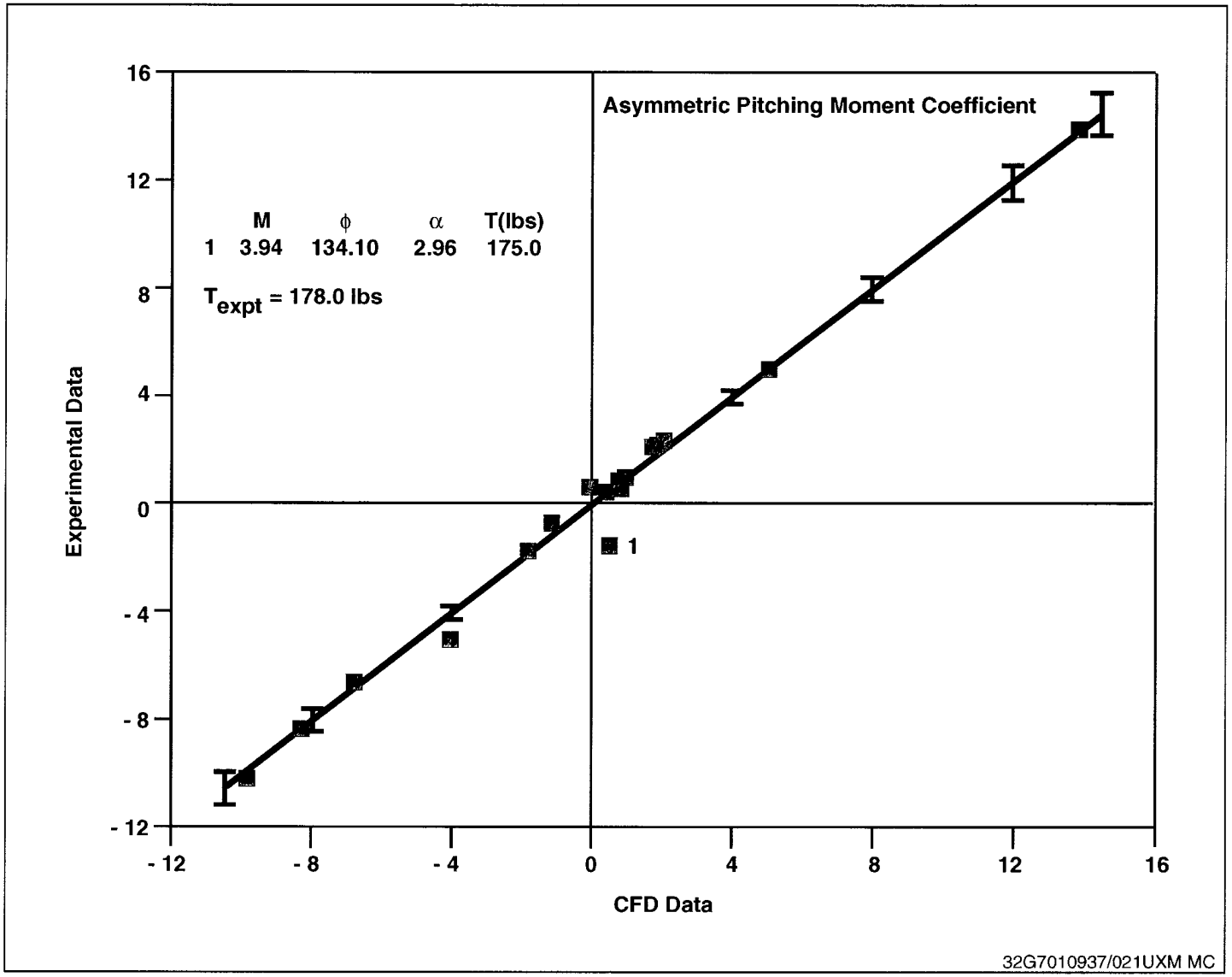

Figure 21. Comparisons of CFD and Wind Tunnel Measurements for an Asymmetric Missile Configuration

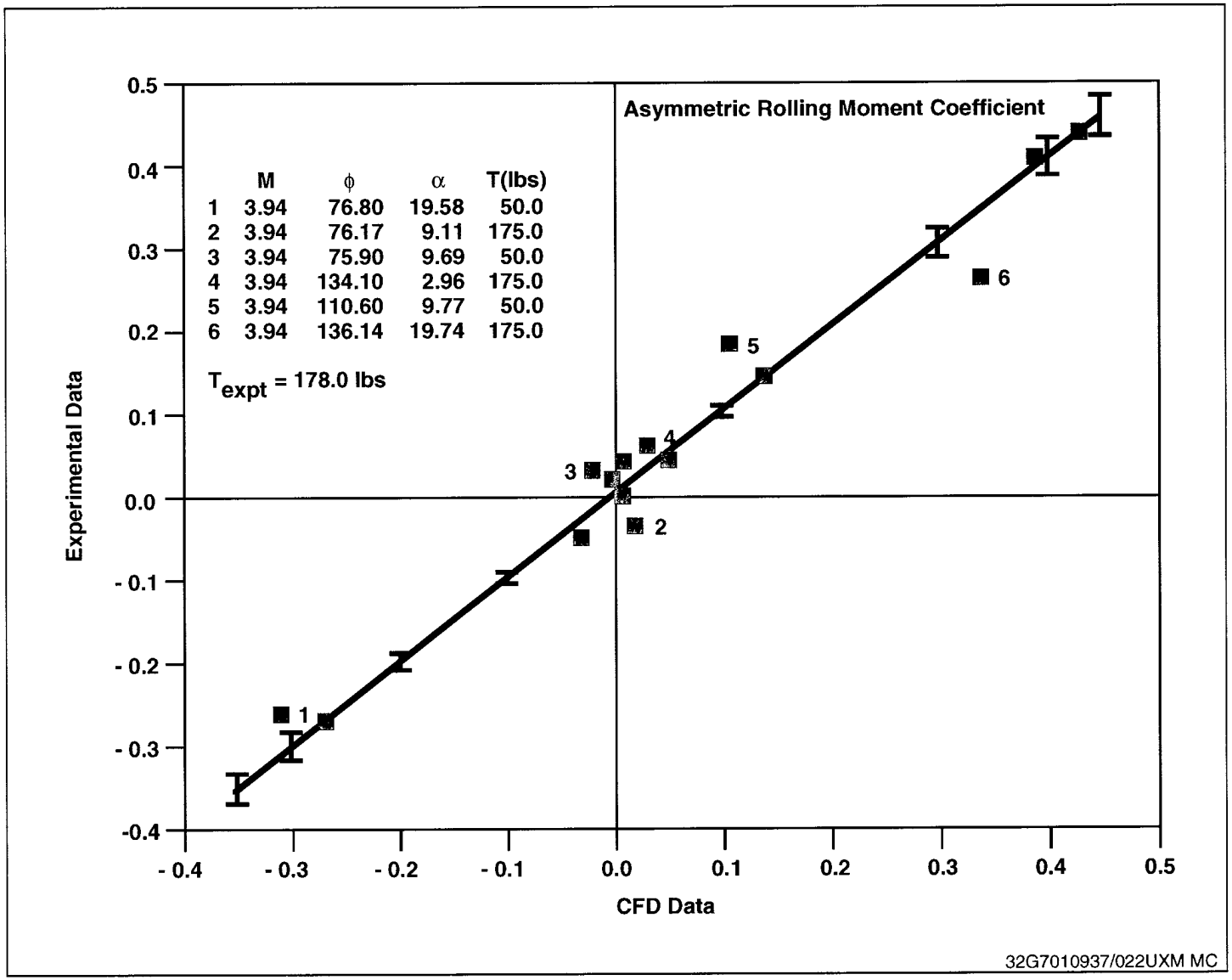

Figure 22. Comparisons of CFD and Wind Tunnel Measurements for an Asymmetric Missile Configuration

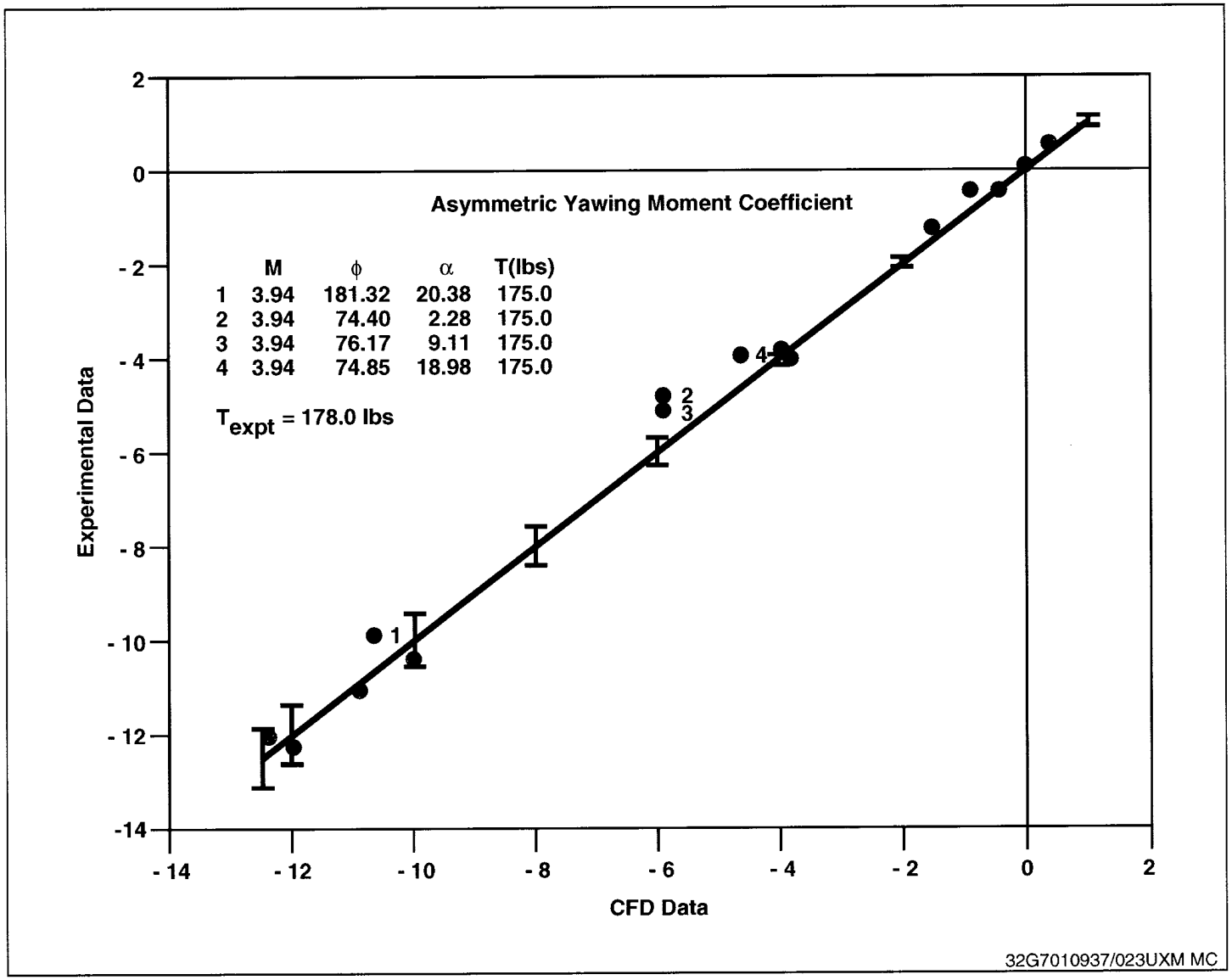

Figure 23. Comparisons of CFD and Wind Tunnel Measurements for an Asymmehic Missile Configuration